> 10^{12}eV

SPECTRA, ANISOTROPIES AND COMPOSITION OF COSMIC RAYS ABOVE 1000 GeV

John Linsley

Department of Physics and Astronomy
University of New Mexico, Albuquerque, NM 87131, USA

ABSTRACT

Updated summaries are given of results on 1) the equal-energy primary composition from charge-resolved energy spectra, 2) the all-particle energy spectrum, 3) N_{max} and N_μ spectra, and 4) harmonic components of the sidereal time variation. Recent results on the energy spectrum of air shower muons are combined with the N_{max} and N_μ spectra in a new synthesis which yields empirical relations for converting N_{max} and N_μ to primary energy. Using these relations a new calorimetric all-particle spectrum is obtained. Ground level data on the primary mass composition at air shower energies, newly analyzed in terms of the average logarithmic mass and the logarithmic mass dispersion, are shown to support a model in which a rigidity cutoff of low energy cosmic rays is masked by proton enhancement beginning before the all-particle knee.

INTRODUCTION

"My task", I began by saying, "is to report on the 10 papers of session OG 4, which was devoted to the topics of this title, and on 2 out of 19 papers in session EA 4, on Optical and Radio Emission from EAS. I was also assigned 8 other EA papers that are concerned with the high energy composition problem, and agreed to do a couple of OG 8 papers on the origin of the highest-energy cosmic rays. That leaves at least 4 other OG papers which were also concerned with the origin of this fraction. I don't know where one draws the line."

"When I got a chance to look at all of the EA papers I found another 15 about composition. That means there are at least 15; my scanning efficiency probably wasn't 100%. I could attend only a few of the MN sessions, but there also I noted a half-dozen papers concerned largely or in part with the same problem. Assuming that people wouldn't spend effort on this problem unless they believe it can eventually be solved, I think the numbers are encouraging. The number of scientists engaged in this study must be at least a hundred."

"To a great extent studies of these topics, the ones listed in my title, depend on using air showers. If one would write 10^6GeV instead of 10^3, that would be entirely true. But the cosmic ray spectrum extends upward another 5 decades, past 10^{20}eV! It's a large field, and a lot is going on here, as I hope to show."

"If I add to all of the papers marked OG those EA and MN papers about composition, I get a grand total of nearly 200. Fully a third of them are concerned with evidence above 10^3GeV, nearly all of it from air showers. Another third are concerned with galactic cosmic rays of lower energy, mostly with the elemental and isotopic composition of the nuclear component, and the rest are theoretical. Some very exciting results in the XG sessions were also obtained using air showers, and I suppose these are the ones that are most challenging of all to theorists. So in spite of notable achievements at lower energies by the use of space vehicles, I would say that there has been a marked trend, over the past decade or so, in favor of the higher energy region."

"The cosmic rays I am going to talk about, with energy per particle greater than 10^3GeV, carry information that promises to be indispensable for deciding between theories of the origin of galactic cosmic rays. Also, they may provide especially direct evidence on the magnetic field structure of the galaxy, out to distances of some kiloparsecs from the solar system. And some of these cosmic rays, having energies greater than 1 joule, appear to be extragalactic. There are difficulties, challenging difficulties, in imagining an astrophysical setting in which acceleration to such great energies can occur at all. And the amount of energy required to fill up the local supercluster with these particles at the observed level of intensity is quite considerable. These extragalactic cosmic rays carry information about the magnetic field between galaxies, and also the radiation field, the photons, out to distances of order tens of megaparsecs or even further."

At that point I described in rather general terms some of the outstanding new contributions, and promised that as soon as I returned to New Mexico I would prepare a written review in which I would try to do better justice to this material, to its quantity and quality. The following pages are in fulfillment of that promise.

It is my second venture of this kind; the first was for a symposium held in Bologna a few years ago (Linsley 1981). More recent reviews of these cosmic ray observations have been given by A. M. Hillas (1981, 1983). Hillas has also done a good deal of work on interpreting this evidence in the light of what else is known about our galaxy, other galaxies, and the intergalactic medium (Hillas 1982). For views which frequently differ from his, and from the views expressed here, see a work by Atrashkevich et al. (1983) presented at last year's European Symposium in Rome.

In Part 1 I describe evidence on the charge-resolved energy spectra of various primary nuclei given by a great many experiments carried out above the atmosphere using balloons and lately satellites. From this evidence I derive improved estimates of the composition for equal energy per particle, vs energy per particle. The subject of Part 2 is the all-particle energy spectrum. In Part 3 I discuss senses in which the primary composition can be measured by various ground level and underground experiments. In Part 4 I offer a proposal for reconciling the all-particle spectrum with the charge-resolved spectra, and I show that it helps to explain some otherwise puzzling features of the indirect evidence on composition. Part 5 is a summary of what is known about the anisotropy, Part 6 is about the neutral primaries, neutrinos and γ-rays, and Part 7 describes some technical developments. Part 8 recalls a few early results that were milestones in the study of air showers.

1. CHARGE-RESOLVED ENERGY SPECTRA

This subject was last reviewed in relation to the all-particle (energy per nucleus) spectrum by Juliusson (1975). Evidence obtained since then indicates that the proton spectrum is less steep and the iron spectrum is less flat above 10^3GeV than seemed to be the case at that time. Figure 1 shows the more recent evidence. If the scale extended to lower energies it would be seen that the proton spectrum hooks downward in much the same manner as the Fe spectrum does here, at about the same energy per nucleon. The spectra of all the elements, insofar as they have been measured to date, at the top of the atmosphere or above it, are well explained by a simple leaky box model with a rigidity dependent mean escape length proportional to $R^{-\alpha}$ with $\alpha \sim 0.5$ (Koch et al. 1981). This model assumes that all elements present at the source start out with the same spectrum, approximately a power law in the total energy (kinetic + rest mass). According to this 'standard model' the spectra of the primary elements at arrival will approach the same form, a power law with an exponent larger by an amount α than at the source (Lezniak and Webber 1978). The data for energy per nucleon < 10 GeV are consistent with an escape-modified spectral index ~ 2.6. Measurements of the He spectrum indicate that this value increases with energy, becoming ~ 2.8 for energy/nucleon 10^2-10^5GeV (Ryan et al. 1972, Burnett et al. 1983 and conference paper OG4-5). In this model the rising portion of the Fe spectrum in Fig. 1 is a propagation effect; it is predicted that above $\sim 10^3$GeV/particle the spectrum will turn over as indicated schematically by the dashed line. As the figure shows, it cannot be proven with existing data that the model is correct in this respect, but the model is a very attractive one. The dotted line through the proton data has the same slope (~ 2.7) below $3\cdot10^4$GeV. The anomaly assumed here above that energy will be discussed in Part 4. The cosmic ray source composition calculated using the standard model resembles the composition of solar material (Shapiro and Silberberg 1975 .

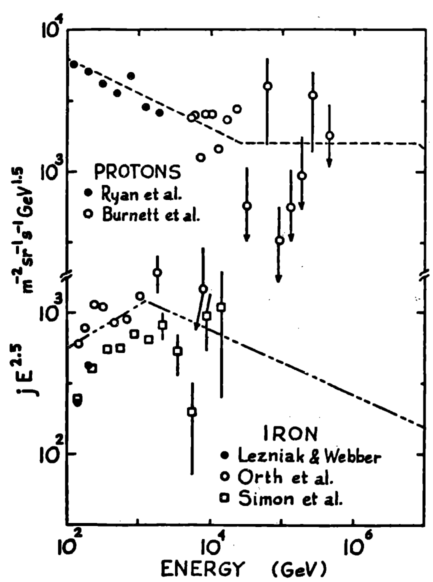

Fig. 1. Spectra of protons and Fe nuclei.

Before the elemental spectra had been measured over a very wide range the equal-energy mass distribution was estimated from the relative abundances at a given rigidity, assuming that all the spectra are power laws with the same index (Ginzburg and Syrovatskii 1961). This distribution is important for interpreting air shower experiments because in these experiments one measures the entire energy of the incident particle, not the energy

Table 1. *Equal-energy mass spectrum of cosmic rays*

energy (GeV)	reference	% element or group of elements: H	He	CNO	10-20	Fe	<ℓnA>	$\sigma_{\ell nA}$
10	Juliusson 1975	58	28	8.3	4.0	1.2	0.79	1.06
10^2	Juliusson 1975	47	25	13.3	10.3	4.5	1.21	1.32
"	present work	54	25	11.4	7.8	2.0	0.98	1.20
10^3	Juliusson 1975	42	20	14.6	14.	10.	1.52	1.47
"	present work	43	19	13.9	15.1	9.6	1.50	1.48
10^4	Juliusson 1975	24	15	37		24	2.26	1.50
"	present work	38	19	13	16	14	1.68	1.53
Ginzburg & Syrovatskii (1961)		43	23	12	14	8	1.41	1.43
Rasmussen 1975 (Shapiro & Silberberg + γ = 2.6)		43	21	13	11	13	1.51	1.51
Shapiro & Silberberg + γ = 2.8 (present work)		31	19	16	14	20	1.94	1.55
Hillas 1983		42	21	13	10	14	1.52	1.52
Ellsworth et al. 1982		55	21	16		8	1.08	1.38
Yodh 1981 (model III)		40	14	11	16	19	1.76	1.63
Abulova et al. 1983		34	20	16	17	13	1.77	1.49

The first 7 rows (Juliusson vs present) give values derived from balloon experiments, showing the trend since 1975. (The new values above 10^2GeV depend heavily on a single experiment by Simon et al. The old values above 10^2GeV depended heavily on a single experiment by Juliusson.)

The Ginzburg & Syrovatskii composition is included because it is well known and used widely. It is remarkably close to the observed composition at 10^3 GeV, both as given in 1975 and as confirmed by later experiments.

The next 2 rows assume a source composition given by Shapiro & Silberberg (1975) and a universal power-law rigidity spectrum with differential exponent as shown. Lezniak & Webber (1978) report data indicating that the source abundance of Fe-group elements may be somewhat greater than assumed here.

The last 4 rows show what the authors named have used in recent published work as corresponding to the low-energy (balloon experiment) data. The model used by Hillas is in good agreement with the extrapolated composition for γ = 2.6. The Yodh model agrees with the latest observations at 10^4GeV within the experimental errors.

per nucleon. Because of propagation effects, the fact for example that low energy Fe is severely attenuated by fragmentation in collisions with interstellar gas atoms, it is better to start with the relative abundances at the source (Rasmussen 1975). In Table 1 I show the results of such calculations, the results of Ginzburg and Syrovatskii, the results obtained experimentally at a number of energies, and some distributions (mass spectra) that have been assumed in air shower simulation work.

At this conference evidence provided by the HEAO-3 satellite experiments continued to pile up. Among the final results of that work will be an Fe spectrum extending to $\sim 4\cdot10^3$GeV with greatly reduced statistical errors, and refined values for the standard model referred to above. In addition, one of the conference abstracts (OG1-15) describes a balloon experiment (HEGCS) designed by Streitmatter et al. to measure the Fe spectrum up to 10^4GeV per particle by means of a gas Cerenkov counter, but as yet there are no results.

Preliminary results are given from two experiments using emulsion chamber calorimeters carried to great heights by balloons: OG4-2 by a group at Moscow State University and OG4-5 by the JACEE collaboration. The results are similar except for protons. The JACEE proton spectrum is shown in Fig. 1. With roughly equal exposures of 80-100 m^2sr hr the MSU group reports finding only one proton with $E > 5\cdot10^4$GeV compared to $\sim$ 10 found by the JACEE group.

Using a novel method for detecting 10^5GeV Fe nuclei at the top of the atmosphere, Sood finds that the intensity is no greater than predicted by the standard model (dashed line in Fig. 1; conference paper OG4-9 and 1983 preprint).

2. THE ALL-PARTICLE ENERGY SPECTRUM

2.1 Review. In recent years substantial advances have been made in the study of this important cosmic ray characteristic. The changes are not so much in the prima facie results as in their trustworthiness. They hardly show in Figure 2, where I have summarized the best available evidence. In this section I first describe and explain such changes as there have been since my previous review. Then I explain the experimental basis for confidence that Fig. 2 is substantially correct in the air shower region as well as in the region investigated using balloons and space vehicles. Note that in deference to the good example set by Hillas, the spectrum shown is a *differential* spectrum. Compared to the summary I gave in 1981 the following changes have taken place:

1) The 'sum' spectrum, given by adding together the charge-resolved spectra where they are available, is more accurate and extends to higher energies. There is good agreement with the Proton Satellite results. However I have disregarded the two highest-energy points given by Grigorov et al. (1971a) because of the large stated errors and the fact that the signals were nearly as large as the design limit. The values shown are derived

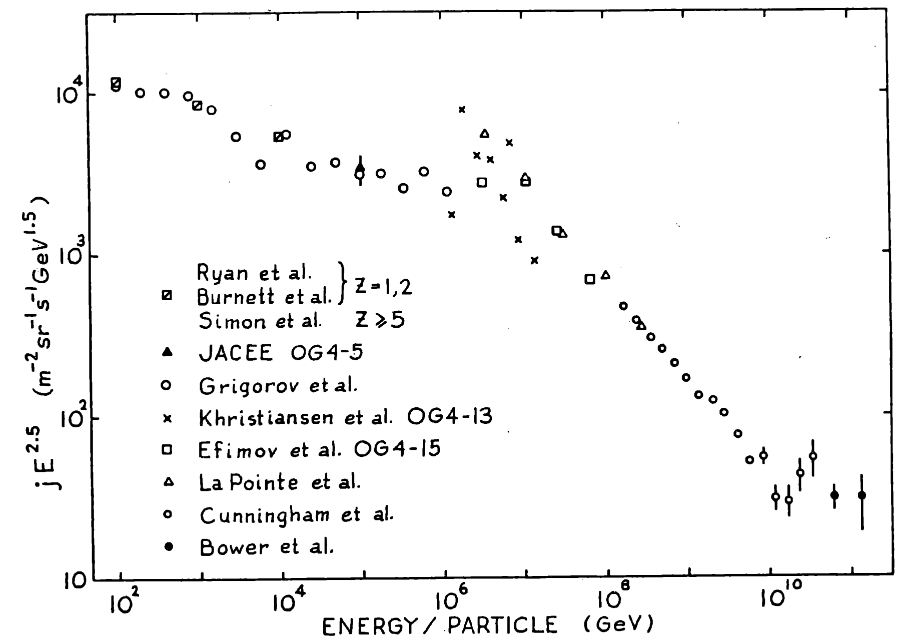

Fig. 2. The all-particle energy spectrum

from Fig. 2 in the second Hobart Conference paper on this subject (Grigorov et al. 1971b).

2) In the small air shower region, 10^6-10^8GeV, I have omitted two early calorimetric points (see Part 8) in favor of results reported at this conference using methods that have special merit (Khristiansen et al. OG4-13 and Efimov et al. OG4-15). Both of them rely on atmospheric Cerenkov light for determining E_{EM}, the energy dissipated by electrons. In one case (Khristiansen et al.), Cerenkov signals are also used to define the acceptance. This is important for reducing the chance of bias due to fluctuations when such small showers are studied at sea level. The preliminary results (x's) scatter a good deal, but eventually this experiment ought to give the best results obtainable at sea level in this region.

3) Alternatively, E_{EM} can be derived from N_{max}, where the shower size N is measured using an array of particle counters. Even at Chacaltaya, the highest suitably equipped ground level station, this can be done without extrapolation only for $E > 10^7$GeV. Higher altitudes can be reached using balloons and aircraft (Antonov et al. conference paper EA1.1-14 and references therein) but then there are other problems (Stamenov and Ushev 1977). Out of the 6 differential points that can be derived from the integral N_{max} spectrum of La Pointe et al. (1968) only the 4 highest-energy ones correspond to well defined maxima. One more point is shown in Fig. 2 but it is uncertain.

4) The 4 highest-energy points in the Haverah Park differential spectrum

(Cunningham et al. 1980) have been replaced by two points derived from integral data by Bower et al. (1983). The reduced statistical errors result from adding in high energy events observed at Haverah during 1980-1983 and at Volcano Ranch during 1959-1963.

Two features of the all-particle spectrum call for some additional comment, the knee and the ankle. Figure 3 shows the region containing the knee. The solid curve is the line I would be inclined to draw through the data points of Fig. 2. The dashed curve is the corresponding line from my 1981 review. The dotted curve is the corresponding line given by Hillas in his most recent reviews (1982, 1983).

2.2 The knee. Why is there such a difference between the latter two, in the small air shower region, 10^6- 10^8GeV? Prior to this conference the most direct evidence by far was from the experiments at Chacaltaya. In this case deriving E is a 2-step process: one first determines N_{max} and then converts from N_{max} to E. On the basis of calculations using an up-to-date cascade model Hillas says that in this energy range the conversion factor should be 1.4 GeV/particle, not 1.6 GeV/particle, the value used in plotting Fig. 2, taken from one of the figures in La Pointe et al., attributed there to calculations by Tanahashi. As I will show further on, the lower value appears to be better; however the difference is quite small, less than 15%.

The main reason for the disagreement between the dotted curve and the solid one in Fig. 3 relates to the experimental problem of measuring N_{max}. It is well known that the data of La Pointe et al. disagree, as to shower size for a given intensity, with results from lower elevations, when the comparison is made for equal depth of shower development (inclined showers at Chacaltaya vs vertical showers at lower elevations). Hillas attributes this disagreement to a θ-*independent* error in the Chacaltaya size values, where θ is the zenith angle. Considering the experimental difficulties in measuring the size of very inclined showers (sea level corresponds to θ ∿ 60° at Chacaltaya); noting also that the disagreement is less between Chacaltaya and Tien Shan (which is at an intermediate depth), I interpret the disagreements to an error which is θ-*dependent*. Since the La Pointe et al. N_{max} spectrum is based on measurements of nearly verti-

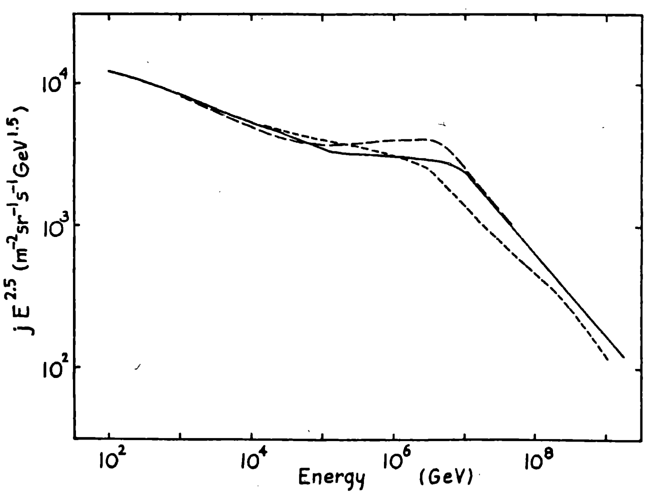

Fig. 3. Comparison of all-particle energy spectra up to and including the knee. The long-dash line is from my 1981 review; the short-dash line is by Hillas (1982, 1983). The solid line is a best fit, by eye, to the data of Fig. 2.

cal showers I see no reason for attempting to correct it as Hillas has done (Hillas 1978). The new atmospheric Cerenkov results from Yakutsk and Samarkand are in good agreement with La Pointe et al. for 10^6-10^8GeV, differing only below 10^6GeV where the Chacaltaya result is recognized to be unreliable (because maximum size is not yet attained at that level).

The question, what value to use for the N_{max} to E conversion factor, merits further discussion because it is related to measurements of air shower muons, in particular to muon size spectra and their application for investigating the all-particle energy spectrum. Before going into that area, however, I will comment on conference paper OG4-21 by Bower et al. relating to a controversy about the highest-energy region in Fig. 2. (As a co-author of OG4-21 I am a party in the dispute; for the opposing view see a review by Atrashkevich et al. 1983 already mentioned.)

2.3 The ankle. Figure 4 shows that there is a substantial disagreement between the combined results of the Haverah Park and Volcano Ranch experiments and a recent result from the Yakutsk experiment (Atrashkevich et al. 1983). The disagreement below 10^{19}eV is small enough to be unimportant. Above $\cdot 10^{19}$eV, however, there is only one event observed, in this data-set from Yakutsk, where 11 ± 2 were expected according to the other two experiments.

The latter both give evidence of a flattening of the primary spectrum above 10^{19}eV, the so-called 'ankle' feature. At least 7 air shower primaries have been assigned energies > 10^{20}eV, and no evidence has been found for a cutoff, predicted on certain models of cosmic ray origin, due to collisions with photons of the cosmic blackbody radiation. The new Yakutsk spectrum, based on an exposure ∿ one third of the Volcano Ranch and Haverah Park experiments combined, indicates that the largest well-measured event had an energy of only $4 \cdot 10^{19}$eV. It shows a cutoff, beginning ∿ 10^{19}eV, of just the sort that interactions with the blackbody radiation would produce, on models that many astrophysicists would like to believe if they were allowed to by the cosmic ray evidence. At stake is a considerable body of work on interpretation of the energy spectrum and anisotropy of the highest energy cosmic rays (see for instance Strong et al. 1974, Giler et al. 1980, and reviews, especially the one by Hillas, 1982). The question is also an important one for cosmology, as shown by reference to it in the invited talk by Narlikar at this conference.

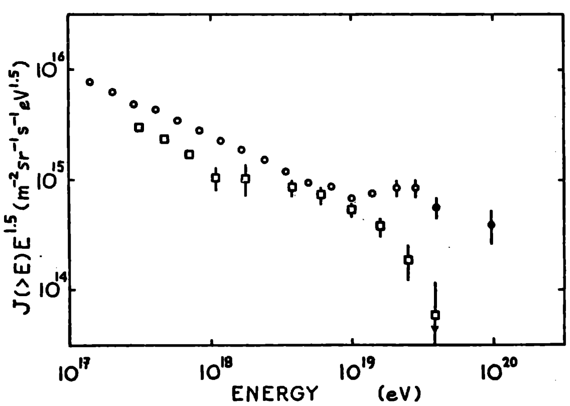

Fig. 4. *Comparison of integral all-particle spectra above 10^8GeV. The circles, open and filled, belong to the same data as in Fig. 2. The squares, taken from paper OG4-21, are a recent result by the Yakutsk group.*

Paper OG4-21 appears to

remove the a priori most likely explanation of the disagreement by showing that the 3 experiments agree closely in relating the respective ground parameters, all of which are different, to the primary energy. In a Yakutsk preprint given to me at this conference it is shown that in certain actual cases the standard procedure used for data reduction by the Leeds group gave a value for ρ_{600}, the Leeds ground parameter, that may have been too high, but in other cases it is conceded that the uncertainty in ρ_{600} is nil (Efimov and Pravdin 1983). In this situation it's the average that counts. The discussion relates to detailed maps showing the particle density recorded by each detector of the array, published in the *Catalogue of Highest Energy Cosmic Rays* (1980) for the largest events registered at Volcano Ranch and Haverah Park. One concludes that possible size-dependent bias in the procedure for evaluating the ground parameter is much too small to explain the disagreement. Is it possible that during the time this data-set was accumulated the Yakutsk selection criteria were overly strict, for the largest showers, so that events were lost?

2.4 Measurement of energy in the air shower domain. My next subject is the accuracy of various primary energy estimates in the air shower region. Of the 3 ground parameters discussed in OG4-21, the one that was used first, at Volcano Ranch, is the shower size assuming an average LDF (lateral distribution function). When the primary data, scintillator densities, from a widely spaced array are fitted in this way the resulting fictitious size is expected to fluctuate much less than the true size with respect to the primary energy. One expects this fictitious size to be about proportional to S_{600}, the scintillator density at 600 m core distance, which is the ground parameter used in the Yakutsk experiment. The ground parameter at Haverah, ρ_{600}, is similar to S_{600} except that it refers to signals from deep water-Cerenkov detectors.

The Volcano Ranch fictitious size is related to primary energy by a phenomenological shower profile model ('longitudinal trial function') which serves two purposes: 1) it relates the fictitious size at the array to N_{max}, the size at maximum development of the same shower assuming that it had the standard profile, taking into account the inclination of the shower and the energy dependence of the average profile; 2) it relates N_{max} to E. Conceptually, the approach is very close to the one used by La Pointe et al.

The Haverah ground parameter is related to primary energy through cascade simulations based on a series of interaction models (Hillas et al. 1971).

The relation of the Yakutsk ground parameter S_{600} to primary energy depends mainly on measurements of the atmospheric Cerenkov light intensity, integrated over the ground plane in much the same way that the particle density is integrated to give the shower size. With proper calibration and due allowance for losses due to atmospheric attenuation this method gives the track length integral of the electrons--the integral of the electron profile--from the start of the shower to the observation level. Therefore, with a usually small correction for energy retained by the soft component when it reaches the observation level, this method gives E_{EM}.

N_{max} and E_{EM} are closely related by phenomenological considerations. It is well known that for cascades initiated by single electrons or photons

$$N_{max} \sim \frac{0.31\ E_{EM}/\varepsilon}{\sqrt{\ln(E_{EM}/\varepsilon)}} \qquad (1)$$

where ε is the critical energy. This equation is approximately true for air showers, requiring only a small correction for differences in elongation and profile width (Linsley 1983a to be published). This is shown by Table 2.

Table 2. Values of the maximum size to energy conversion factor for electromagnetic cascades and the air shower soft component.

E_{EM} (GeV)	10^5	10^6	10^7	10^8	10^9	10^{10}
E_{EM}/N_{max} | Eq. 1	0.98	1.06	1.13	1.20	1.26	1.32
E_{EM}/N_{max} | EAS	0.93	1.00	1.06	1.12	1.17	1.22

In making the correction it is assumed that x_{max} = 159 + 65 log E (GeV) (Linsley and Watson 1981) and that $\sigma_x^2 = 1.1 \cdot 10^4 + 4.2 \cdot 10^3 \log E$, where x_{max} and σ_x are in g/cm^2 and E is in GeV. For experimental evidence supporting the equation for σ_x see Grigoriev et al. conference paper EA4-4.

The distinction I have been making between E and E_{EM} is especially important for small showers. At all air shower energies most of the primary energy is given, via π_o decay, to the electromagnetic component, but a portion is given to muons and deposited at great depths, and another portion is given to neutrons and deposited, often tardily, at large lateral distances. Most of this energy is overlooked in measuring the track length integral, by whatever method this is done. A portion of the primary energy is deposited by particles with 'black' or 'grey' tracks in the parlance of emulsion work, a portion is consumed by endothermic nuclear reactions like the one responsible for ^{14}C, and a portion is given to neutrinos. This energy also is missed or under-weighted.

To allow for all these processes one can write $E = E_{EM} + E_{\mu\nu h}$. Then the over-all conversion factor is given by

$$\frac{E}{N_{max}} = \frac{E_{EM}}{N_{max}} / \left(1 - \frac{E_{\mu\nu h}}{E}\right) \qquad (2)$$

It follows from (2) and Table 2 that a discussion of the conversion factor amounts to a discussion of the fraction $E_{\mu\nu h}/E$. *Whether on the one hand N_{max} is measured, or on the other, atmospheric Cerenkov light is used to find E_{EM} directly, the conclusion is the same: at present, the uncertainty in determining primary energy by means of air shower techniques is essentially the uncertainty in our knowledge of $E_{\mu\nu h}$.* If there is some kind of Urca-process peculiar to the air shower region, which converts primary energy into neutrinos with great efficiency, then of course the primary energy can be *under*-estimated by any amount. But if available techniques are used properly there is no way that the primary energy can be over-estimated by more than the amount that $E_{\mu\nu h}$ may be over-estimated.

2.5 Conversion factors; the importance of muon data. Returning to the small air shower region, one can now ask whether at these energies the fraction $E_{\mu\nu h}/E$ is equal to 30-40%, consistent with 1.6 GeV/particle, the old value of the conversion factor, or is it equal to 20-30%, as Hillas's new value implies? Is it necessary to resort to interaction models, or can this question be decided experimentally?

In an experimental approach the most important steps are to measure the number of muons N_μ (above some muon energy threshold usually $\sim$ 1 GeV), and the energy spectrum of these muons. In this way one obtains $E_{\mu,obs}$, the total energy of muons reaching the observation level. To obtain the energy given to neutrinos these muons are propagated backward to a production spectrum. In the air shower region it is found that $E_\nu \sim 0.4\ E_{\mu,obs}$, where E_ν includes both ν_μ and ν_e. This result checks with a forward-propagation calculation by Hillas (1981). Experiment-based estimates of E_h, the energy given to low-energy hadrons, range from 0.8 $E_{\mu,obs}$ (Greisen 1956) to 0.3 $E_{\mu,obs}$.

Studies of both the number and energy spectra of air shower muons began in the 1950's and still continue. At this conference muon size spectra are reported by groups from Akeno (paper OG4-16) and Sydney (paper EA1.2-15). Information relating N_μ to scintillator size N_s and primary energy is presented by the Yakutsk group (paper EA1.2-12). Results on the muon energy spectrum will be published by Atrashkevich et al. in a late volume (conference paper EA1.1-34). A comparison of results on N_μ's is made in Table 3. On the whole the agreement is remarkably close. At an intensity of 10^{-11}/m^{2}sr s, where the new results overlap several previous ones, it appears that the SUGAR (Sydney) N_μ-values may be $\sim$ 25% high while the 1979 Yakutsk values may be low by an equal amount. By combining these results with some N_μ data obtained earlier at Moscow State University (Vernov and Khristiansen 1968) one finds that over a very wide range of integral intensities, 10^{-6} to 10^{-17} /m^{2}sr s, they can be represented well by a simple power law,

$$J_\mu(>1\text{GeV})_{\text{sea level}} = 3\cdot 10^4\ N_\mu^{-2.4} \ . \qquad (3)$$

For the purpose of this comparison the Akeno and Volcano Ranch results are adjusted to sea level using an attenuation length of 1440 g/cm^2 (Diminstein et al. 1983). The MSU result is adjusted to a 1 GeV threshold using Khrenov's formula (Khrenov and Linsley 1981); otherwise a simpler formula due to Greisen is used (Greisen 1960). For $J \leqq 10^{-14}$, Eq. 3 agrees with the average observed N_μ within 10% or less; at lower intensities, where there is no cross-check, it disagrees by 20-25% with the formula used by the Sydney group to represent its N_μ spectrum.

Recalling Table 2, the one which relates E_{EM} and N_{max}, one may notice that it would be possible, using it, to convert the observed N_{max} spectrum of cosmic ray showers to an E_{EM} spectrum. So one may ask, can the N_μ spectrum

Table 3. Muon size for a given intensity observed in various experiments

integral intensity	muon threshold	N_μ (>1GeV)	reference
$10^{-6}/m^2 sr\ s$	10.0 GeV	2.3×10^4	Vernov & Khristiansen 1968 (*)
10^{-7}	"	6.5 "	"
10^{-8}	10.0	1.6×10^5	"
"	1.0	1.6 "	Hara et al. 1983 (@)
10^{-9}	10.0	3.8 "	Vernov & Khristiansen 1968 (*)
"	1.0	4.0 "	Hara et al. 1983 (@)
10^{-10}	1.0	1.0×10^6	"
10^{-11}	0.22	2.5 "	Linsley 1973 (@)(#)
"	0.70	2.0 "	Diminstein et al. 1979 (#)
"	0.75	3.5 "	Horton et al. 1974 (#)
"	1.00	2.4 "	Dixon et al. 1974
"	1.00	2.6 "	Hara et al. 1983 (@)
10^{-12}	0.70	5.7 "	Diminstein et al. 1979 (#)
"	0.75	9.2 "	Horton et al. 1983 (#)
10^{-13}	0.70	1.6×10^7	Diminstein et al. 1979 (#)
"	0.75	2.4 "	Horton et al. 1983 (#)
10^{-14}	0.75	6.4 "	"
10^{-15}	"	1.7×10^8	"
10^{-16}	"	4.5 "	"
10^{-17}	"	1.2×10^9	"

(*) *adjusted to 1 GeV threshold by means of Khrenov formula (Khrenov and Linsley 1981)*

(#) *adjusted to 1 GeV threshold by means of Greisen formula (Greisen 1960)*

(@) *adjusted to sea level assuming attenuation length 1400 g/cm²* *(Diminstein et al. 1983)*

be used in a similar manner? Can it be converted, without using an interaction model, to an $E_{\mu\nu h}$ spectrum? In the next paragraph I will show that indeed this can be done. Combining the two, one obtains the all-particle energy spectrum.

It has been shown by Khrenov that as in case of N_μ there is also good agreement among independent measurements of the energy spectrum of air shower muons (Khrenov 1981 unpublished report, Atrashkevich et al. EA1.1-34). This spectrum is quite hard; almost half of the observed energy is given to particles with individual energies above 30 GeV. Over the energy range where it has been studied ($3\cdot10^5$-10^8GeV) the shape of this spectrum is invariant; hence the total energy of the observed muons is proportional to $N_\mu(>1\text{GeV})$, where the experimental value of the proportionality constant equals 10.0 ± .5 GeV. Recalling that $E_\nu \sim 0.4\ E_{\mu,obs}$, and adopting $E_h \sim 0.4\ E_{\mu,obs}$ as a conservative estimate of the energy given to soft hadrons, I obtain

$$E_{\mu\nu h} = (18\ ^{+3.5}_{-1.5}\ \text{GeV})\cdot N_\mu(>1\text{GeV})_{\text{sea level}}\ . \qquad (4)$$

Neither this result nor the one expressed by Table 2 depends on any assumptions about the primary composition; they are properties of cosmic rays *as they occur*, in this energy range, at the solar system. As an experimental result, Eq. 4 applies to the energy range given above, $3\cdot10^5 < E < 10^8$GeV. Extrapolation up to 10^{11}GeV is justified unless some change occurs, affecting the production of *very high energy* muons and neutrinos, which is as radical and unexpected as the Urca process mentioned earlier. By substitution in Table 3, after averaging the experimental N_μ values for each intensity, Eq. 4 gives the promised $E_{\mu\nu h}$ spectrum.

Table 4 is a summary of results on the N_{max} spectrum. Conversion to an E_{EM} spectrum is accomplished by means of the relation

Table 4. Maximum size for a given intensity observed in various experiments

integral intensity	observation depth	x_{max}	N_{max}	reference
10^{-5}/m^{2}sr s	210 g/cm^2	450 g/cm^2	3.5×10^5	Antonov & Ivanenko 1975
10^{-6}	"	490	1.3×10^6	Antonov et al. 1983
"	540		1.3 "	La Pointe et al. 1968
10^{-7}	"		4.2 "	La Pointe et al. 1968
10^{-8}	"		1.15×10^7	La Pointe et al. 1968
"	"		1.30 "	Kakimoto et al. 1981
10^{-9}	"		3.6 "	La Pointe et al. 1968
"	"	550 (*)	4.0 "	Kakimoto et al. 1981
10^{-10}	"		1.05×10^8	La Pointe et al. 1968
"	"	600 "	1.20 "	Kakimoto et al. 1981
10^{-11}	"		3.2 "	La Pointe et al. 1968
"	"	600 "	4.0 "	Kakimoto et al. 1981
10^{-12}	"	650 "	1.26×10^9	"
"	835		$5. \times 10^8$	Linsley 1973
10^{-13}	"		1.6×10^9	"
10^{-14}	"		$1. \times 10^{10}$	"

(*) *These values are included to call attention to the fact that they are ∿ 100 g/cm^2 less than values derived from Cerenkov light profiles.*

$$\log N_{max} = 0.144 + 0.976 \log E_{EM} \quad (5)$$

which represents Table 2 (for EAS) within 2% for E_{EM} in the range 10^5-10^{10} GeV. I will not show the E_{EM} and $E_{\mu\nu h}$ spectra here but will move on to results of a more familiar kind.

By combining Tables 3 and 4 one obtains a wealth of information. Each intensity provides associated values of N_{max} and N_μ. By using Equations 4 and 5 one obtains the corresponding values of E_{EM} and $E_{\mu\nu h}$. Adding them one obtains E. E/N_{max} is the conversion factor from N_{max} to E, which serves to convert Table 4 into an integral energy spectrum. E/N_μ is the conversion factor from N_μ to E. It serves to convert Table 3 into an energy spectrum which of course is the same because the constraint $E = E_{EM} + E_{\mu\nu h}$ forces agreement. So far as the muon data are concerned the resulting spectrum is entirely independent of data shown previously in Fig. 2. For reasons that I will explain later I choose here to adopt the later Chacaltaya results shown in Table 4, rather than those of La Pointe et al. Consequently the new energy spectrum derived calorimetrically from the two tables is almost entirely independent of the one shown earlier. (The results shown in Table 4 for the highest intensity and the two lowest intensities are not used. They are included to encourage further work. The Antonov result at $10^{-6}/m^2$sr s has been corrected for effects pointed out by Stamenov and Ushev (1977); the question of correcting the higher intensity point is still under study by the MSU group. The Volcano Ranch N_{max} values have not been corrected using the more accurate LDF reported in Plovdiv (Linsley 1977); they are certainly too small by about a factor 2.)

The experimentally determined conversion factors are shown in Figures 5 and 6. The one for converting N_{max} to E is even smaller than Hillas's 1.4! It is almost constant over the range shown, from $2\cdot10^6$GeV to $2\cdot10^9$GeV, the average value being 1.3 ± .2. The energy independence is explained by the fact that a slow increase of E_{EM}/N_{max} with increasing primary energy, due to increasing elongation and width of the shower profile, is offset by an increase of E_{EM}/E as more and more of the primary energy goes into soft component.

This trend is shown in Figure 7 together with other experimental points and 3 curves calculated using interaction models. There is good agreement with the calorimetric points by Nikolskii and Zatsepin et al., both of which were based on data obtained at the Pamir mountain station, and with the lower energy points by Atrashkevich et al. The downward trend and the low absolute values given by Atrashkevich

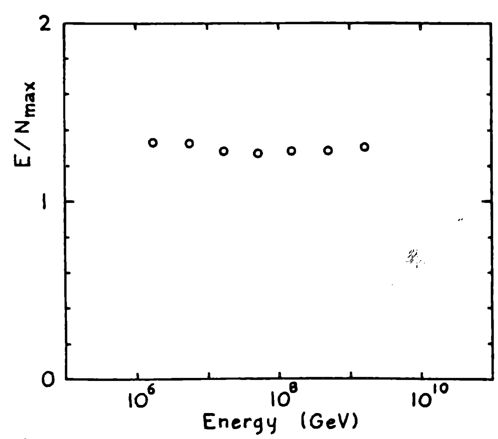

Fig. 5. Maximum shower size to primary energy conversion factor, as a function of primary energy.

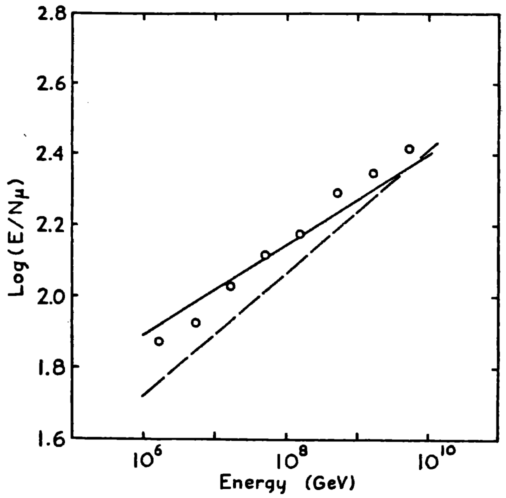

Fig. 6. *Muon size to primary energy conversion factor, as a function of primary energy.*

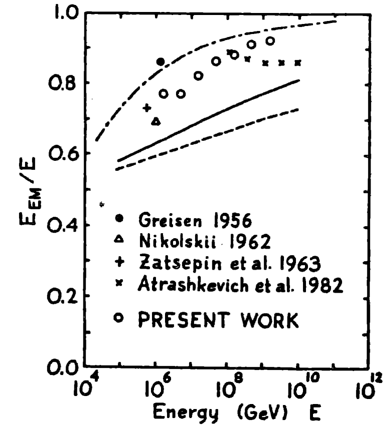

Fig. 7. *Fraction of primary energy given to the soft component, as a function of primary energy.*

et al. at the higher energies must be a reflection of experimental uncertainties in the data that were used. The result by Greisen is too high; the energy given to muons was under-estimated. The solid curve and the dot-dash curve are for models that are both described as 'scaling with constant cross sections', the former given by Gaisser (1979, 1981) and the latter by Hillas (1981). They are shown to point out that the danger in using models for analyzing air shower results is not only that the model may be wrong; it is also that the calculation may be wrong. The model in question is known to give poor agreement with experimental data; for one thing it gives conversion factors that are too large, $E/N_{max} \sim 1.7$. The dashed curve is for a 'high multiplicity' model (Gaisser 1979, 1981).

2.6 New calorimetric energy spectrum. The new energy spectrum is shown in Figure 8, together with a line representing the data of Fig. 2 and one taken from Hillas's reviews. In this comparison the full line can be taken to represent, in the interval $3\cdot10^6$–10^8GeV, the Yakutsk result (OG4-15), which is also calorimetric. At 10^9GeV the full line joins smoothly to the Haverah points.

2.7 Conversion of muon size spectra to energy spectra. In Fig. 6 lines are shown representing two pairs of empirical conversion formulae given in conference papers. The flatter one, which agrees better with the points, is from conference paper EA1.2-12 by Diminstein et al.. In conference paper OG4-16 by Hara et al. a practically identical result is obtained by combining the Akeno N_μ vs S_{600} relation and the Yakutsk S_{600} vs E relation. The steeper one is from two other formulae by Hara et al., one of them obtained by combining the Akeno N_μ vs S_{600} result with the Leeds E vs ρ_{600} relation, using a single measurement of the ρ_{600}/S_{600} ratio. This formula should be disregarded because recent measurements show that the above ratio is energy dependent. The other formula was obtained by adjusting the constants to

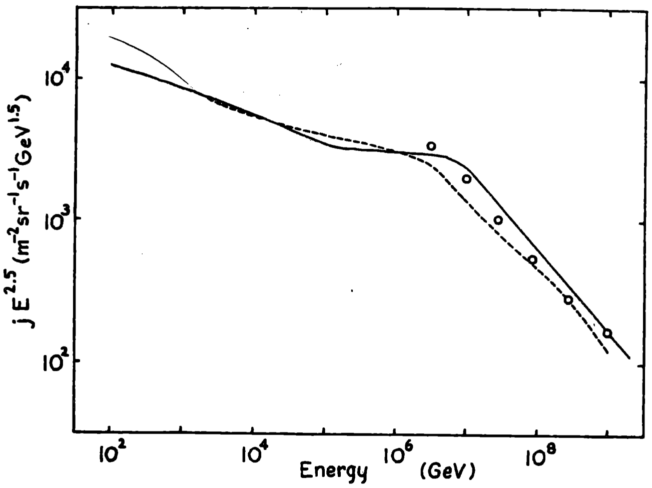

Fig. 8. Calorimetric determination of the all-particle energy spectrum.

bring about agreement between energy spectra derived from the Akeno N_e and N_μ data. The best straight line through the points of Fig. 6, which is preferable to either of the other lines (because based on more evidence and tested over a wider energy range), corresponds to

$$E/N_\mu(>1\text{GeV})_{\text{sea level}} = 6.8\ E^{0.165}, \quad (6)$$

where E is in GeV.

2.8 Southern hemisphere all-particle spectrum. One of the most notable results presented at this conference is the final version of the energy spectrum obtained with SUGAR, the Sydney University Giant Airshower Recorder (Horton et al. paper OG4-20). It depends on measurements of muon size that are included in the Table 3 summary. In converting this to an energy spectrum the authors chose, for the sake of consistency, to use the same formula used earlier in their work, based on a certain interaction model. They will not be surprised to find, when they read this, that I prefer an alternative. Figure 9 shows the SUGAR spectrum assuming that N_μ is given by the formula of Diminstein et al. (the better-fitting line in Fig. 6), with N_μ values adjusted by a factor 1.13 to allow for the difference in threshold energy (0.75 GeV for SUGAR vs 1. GeV for this recent Yakutsk result). The straight dashed line is a best fit to the SUGAR data over the whole range of sizes and zenith angles. The filled points connected by a full line represent the spectrum observed in the northern hemisphere at Haverah Park. At energies below ~ $3\cdot10^9$GeV the Haverah Park-SUGAR difference is accounted for by the 25% discrepancy in N_μ values noted in connection with Table 3.

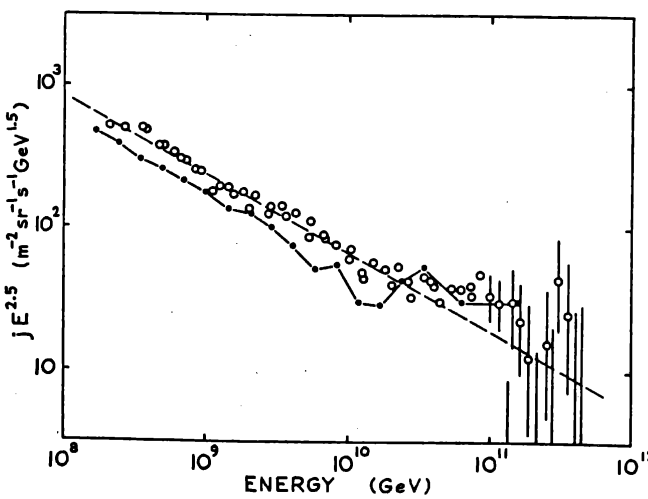

Fig. 9. All-particle spectra in the southern hemisphere (SUGAR, open circles) and northern hemisphere (Haverah Park, filled circles).

Even when the tendency

to overestimate N_μ is taken into account, assuming that it persists to the highest energies, the energy of the largest shower registered in this experiment comes to $4 \cdot 10^{20}$eV, a new high-energy record. In view of the evidence for a strong anisotropy above 10^{19}eV, at least in the northern sky, the energy spectra shown in Fig. 9 are allowed to be different in this region. In fact, whatever difference there may be is less than the experimental errors are, at present. In this region the SUGAR spectrum appears to flatten somewhat, just as the Haverah spectrum does. The SUGAR flattening is stated to be statistically significant at a confidence level of better than 99%.

2.9 Other methods. Another notable conference report is one by the Fly's Eye group giving a preliminary result on the energy spectrum (paper OG4-18 by Cady et al. to be published in a late volume). At present the group is unable to derive from its data the usual sequence of points representing the differential intensity vs E; it uses a Monte Carlo simulation procedure to find best-fitting power law models of the integral spectrum. The result to date, based on ∿ 600 showers with E > 10^8GeV, agrees very closely with the Haverah spectrum. It should be kept in mind however that the Fly's Eye measures E_{EM}, not E. As in case of the Yakutsk and Volcano Ranch experiments, one must make allowance for $E_{\mu\nu h}$, the energy which escapes direct observation. In the Utah analysis, as it has been carried out to date, this allowance is built into the formula used by the group to fit its profile data. Using the same formula I obtained the full line shown in Fig. 7, which deviates significantly from the experimental points. Adopting this formula is equivalent to assuming that the N_{max} to E conversion factor equals 1.7 rather than 1.3. It follows, if I am not mistaken, that the agreement with other experiments is not quite as good as it seems to be. At this stage of technical development the assigned energies are 25-30% higher than they ought to be, which implies, if this is the only problem, that the signals from a given shower are 25-30% weaker, as detected, than the calibration procedure leads one to believe. It would not be surprising if this were the case considering that this new method for determining the absolute value of E_{EM} is so different from the other two methods, one relying on absolute measurements of the atmospheric Cerenkov light, the other on data from arrays of scintillators.

At least in principle the atmospheric Cerenkov technique can be applied over a very wide energy range, beginning ∿ 10^3GeV or even lower (Gerdes et al. 1973). An improved method of detection for the low energy region is described in conference paper OG4-1 by MacKeown et al. but no new results are given. In this case, in addition to problems discussed by these authors, of relating the signals to E_{EM}, the difficulty of estimating $E_{\mu\nu h}$ becomes proportionately greater than at higher energies. As Fig. 7 suggests and as cascade simulations confirm, below 10^5-10^6GeV the correction required is substantial, ∿ 100% of the energy that is observed. The correction term has not been measured experimentally in this range. It is difficult to calculate reliably because it is sensitive to the interaction model. Because of the strong energy dependence of $E_{\mu\nu h}$ in this region, the correction is also sensitive to the primary composition, a problem which is now less serious, in this region, than it used to be.

2.10 The highest energies. There are problems in applying any of the calorimetric methods to the largest showers. The techniques that depend on detecting atmospheric Cerenkov or fluorescent light can be used only on moonless nights in ideal weather, so they are sensitive only 5-10% of the time. Counter arrays are sensitive practically all of the time, but they determine N_{max} on an average basis, requiring a sample of 100 events or so. In case of the largest showers, relative calibrations are used, which are based on various ground parameters: ρ_{600} at Haverah, S_{600} at Yakutsk, a certain fictitious size N_F at Volcano Ranch, and N_μ in case of SUGAR. In many cases these can be cross-checked. The Volcano Ranch data yield S_{600} as well as N_F. There was even a muon detector, albeit a small one, which provided estimates of N_μ. At Haverah, the Leeds group has installed scintillators for measuring S_{600} and there is a fairly large muon detector. The Yakutsk array has even better muon coverage, and in this case a great deal of effort has been devoted to measuring the atmospheric Cerenkov signal whenever possible.

In general these ground parameters depend for their accuracy on correctly estimating the shower impact parameter, R_p, the perpendicular distance of the shower axis from some detector. Especially in case of Haverah, but also in case of Volcano Ranch, a cross-check on the accuracy of R_p is given by the risetime of the signals, in the one case from water-Cerenkov tanks, in the other from scintillators.

2.11 Conclusion. The all-particle energy spectrum has now been determined to an accuracy of about ± 10% over the entire range from energies where solar modulation is the limiting factor up to $\sim 10^{10}$GeV where statistical errors in the number of large showers cause that margin to be exceeded. The spectrum extends well beyond 10^{20}eV. Starting at 10^2GeV, the slope first decreases slightly and then increases markedly at the knee. At $\sim 10^{10}$GeV it again decreases. The portion measured using air showers is summarized in Figure 10 using an alternative description which is more convenient for some purposes than the one used earlier.

The only serious problem is the deficiency of very large showers in the Yakutsk data. What seemed to be a conflict between results from Chacaltaya and from lower elevations has been resolved. The earlier values of N_{max} (La Pointe et al.) were somewhat too *low*, but energies were about correct because the conversion

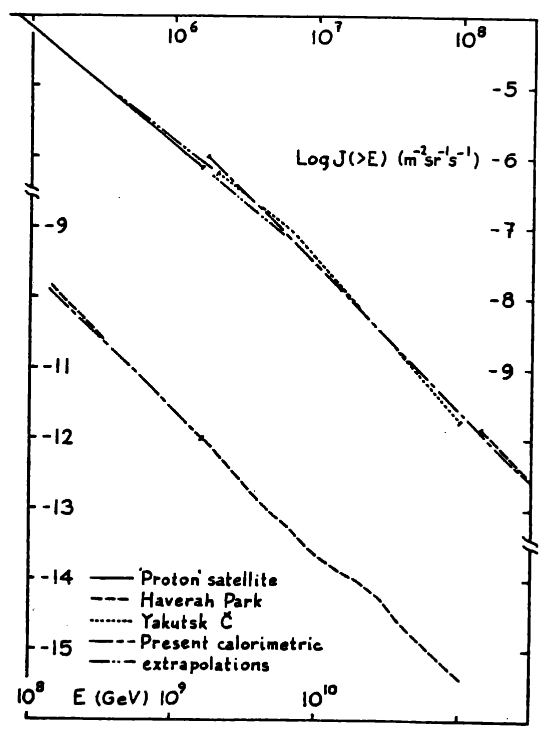

Fig. 10. The integral all-particle spectrum.

factor was somewhat too high. The later values of N_{max} are more nearly correct, but the energies were too high because the conversion factor was *much* too high, 1.8-2.1 GeV/particle (see Kakimoto et al. 1981, Fig's 2 and 4).

2.12 Kinks as evidence of changes in particle physics. There is some kind of mystery relating to the 'kinks' which many phenomenological spectra exhibit at integral intensities in the range 10^{-6}-10^{-7}/m^2sr s. It is noteworthy that the experimentally determined conversion factors E/N_{max} and E/N_μ show no abrupt changes as the knee of the all-particle spectrum is crossed. The existence of a knee, that is, a change in the power law index from $\sim$ 1.6 in the 10^2-10^4GeV region to $\sim$ 2.1 in the 10^8-10^{10}GeV region, cannot be doubted. However the evidence we have is not capable of showing that the change is very abrupt, if it is. The region of most rapid change seems to lie between $5 \cdot 10^6$ and 10^7GeV; it cannot be pinned down more closely than that with present data.

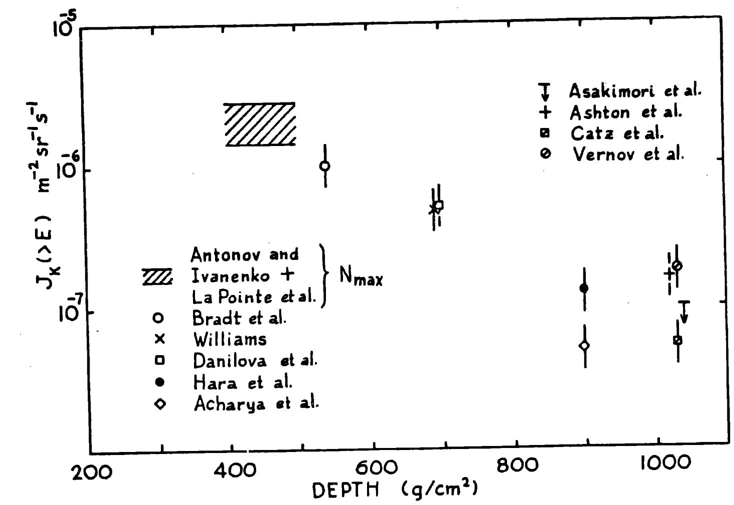

Fig. 11. *Integral intensity corresponding to the size spectrum kink, at various depths.*

The kinks that are seen in phenomenological spectra are often quite sharp. This already causes difficulty in explaining them as due solely to the spectral knee; there are astrophysical arguments that a spectral knee should not be as sharp as that (Bell et al. 1974). Moreover, a kink due solely to the energy spectrum would be sharpest at the highest elevations and would fade away rather quickly at increasing depths because of fluctuations. Another objection, pointed out by Hillas several years ago, is that kinks observed at different altitudes, particularly the kink in the size spectrum, do not correspond to the same intensity, as first thought. Instead, as Figure 11 shows, the size spectrum kink seems to 'propagate' to lower intensities, which means higher energies, as the showers propagate downward in the atmosphere. This suggests that some particle physics threshold may be involved, which governs the *early* behavior of showers made by 10^6GeV primaries (but not their behavior at sea level because it is washed out by fluctuations) and the *later* behavior of 10^7GeV showers, where the behavior at sea level is due to the same threshold being crossed in the third or fourth collision of the leading nucleon.

Shower density spectra also show these kinks. Hillas has argued that this evidence indicates a preponderance just above 10^6GeV of shower primaries having a very short collision mean free path (Hillas 1981). However McGaughan, whose experiments show the clearest evidence of this sort, concludes that the rapid change in exponent of the shower size spectrum, as well as the similar change in the density spectrum exponent, is the expression of an interaction change over and above a relatively gradual steepening of the energy spectrum (conference paper EA3-1 to be published in a late volume). I will not go on to list here other evidence for particle physics thresholds in the energy range $\sim 10^6$GeV; it is well known that there is such evidence.

3. EVIDENCE ON PRIMARY COMPOSITION FROM GROUND LEVEL EXPERIMENTS

3.1 Description in terms of lines; appropriate measures of composition in the air shower domain. The situation in this area of study may seem at first glance to be chaotic; however it can be put in order to some degree, as I will show. All experiments I know of to study the primary composition can be described in classical terms as attempts to determine the relative intensities of spectral lines belonging to the various components. These lines have a certain separation, and they are more or less broadened, due not only to instrumental effects, which I will largely ignore, but also, unavoidably, due to physical processes beyond control. It is a common feature of ground level experiments (I intend the term to include experiments carried out in mines and tunnels or under water), whether they use air showers, high energy muons, or γ-ray families, that the intrinsic breadth of the lines is great; so great in relation to the line separation that at best only broad features can be resolved: protons from alpha particles, for example, but not carbon from oxygen. And in many cases the resolution is intrinsically much worse, so that a proton line could barely be resolved from an iron line of equal intensity, assuming no other lines to be present.

In most cases the line separation is proportional to ln A, where A is the mass number. For this reason, and in general to avoid giving undue importance to elements in the Fe group, it is preferable to use this variable, which I will denote by a, rather than A itself in discussing averages and dispersions. If w_i are the line intensities, normalized so that $\Sigma w_i = 1$, then $\langle \ln A \rangle = \langle a \rangle = \Sigma w_i \ln A_i$, $\sigma^2_{\ln A} = \sigma_a^{\ 2} = \Sigma w_i (\ln A_i - \langle \ln A \rangle)^2$, and so forth. Values of $\langle \ln A \rangle$ and $\sigma_{\ln A}$ are given in Table 1 for the energy region where cosmic ray composition has been measured above the atmosphere with good resolution. Many ground level experiments essentially measure $\langle \ln A \rangle$ or $\sigma_{\ln A}$; others are mainly sensitive to *changes in* $\langle \ln A \rangle$ vs E.

The lines belonging to various components are broadened by fluctuations, primarily by fluctuations in the depth of the initial collision between the primary particle and an air nucleus, but also by fluctuations in subsequent development of the resulting air shower. The magnitude of these fluctuations is primary mass dependent; hence fluctuation measurements afford another approach to studying the composition.

In practice the width of an observed spectrum depends on $\langle \ln A \rangle$ as well as $\sigma_{\ln A}$. This is shown by the following equation derived in the Appendix:

$$\sigma_y^{\ 2} = (\sigma_{\langle a \rangle})^2 + (k^2 \sigma_1^{\ 2} + b^2)\sigma_a^{\ 2} \ . \qquad (7)$$

Here y is an air shower observable whose mean value for proton initiated showers can be graphed vs lnE as a straight line (over some reasonably wide interval; 2 decades is enough), b is the slope of this line (rate parameter), σ_1 is the dispersion of y for proton initiated showers, $\sigma_{<a>}$ is the corresponding quantity for showers initiated by nuclei with average a, where a = lnA, and σ_y is the observed dispersion for a mixed primary composition. The constant k describes the line width for showers initiated by various nuclei:

$$\sigma_i = \sigma_1(1 - ka_i) \quad . \tag{8}$$

It follows from (8) that $\sigma_{<a>} = \sigma_1(1 - k<a>)$. In case of the observables I will be dealing with, the quantity σ_i has been studied by means of cascade simulations using the Monte Carlo method. It is found that the value of k lies in the range 0.15 ± .05, depending somewhat on the model (Elbert et al. 1976, Ellsworth et al. 1982, Chantler et al. 1982). In the remainder of this section I will use Eq. 7 and a companion equation for <y> as ordering principles, to show in some important examples what has been learned so far, what the problems are, and what prospects there are for making more headway in the next few years.

3.2 Fluctuations in xmax. In all cases I will adopt the value 0.15 for k. The first application is to data on x_{max}, the depth of maximum development or elongation. At this conference there are reports by two groups which have been studying the dispersion of the x_{max} distribution: papers EA1.2-10 by Dyakonov et al. and EA1.2-11 by Walker and Watson. These are especially important because they extend to such high energies, $\sim 10^{10}$GeV, and because the observable is comparatively well understood theoretically. The combined results are shown in Figure 12. (Two points with relatively large errors from the 1974 paper by Watson and Wilson have been omitted.)

In this case the rate parameter is just the elongation rate D_e. It can be evaluated using an interaction model, or it can be taken from experimental data on the energy dependence of x_{max}, *assuming only that <lnA> is essentially constant above* $\sim 10^8$*GeV, regardless of what the value of <lnA> may be*. Using the latter approach I will adopt the value 28 g/cm^2 (Linsley and Watson 1981).

For values of the p-air cross section as large as those which seem to prevail here, one expects that in this case σ_1 will be proportional to the p-air interaction mean free path. According to calculations by Walker and Watson (1982) the constant of proportionality is 1.4. Using Glauber theory the p-air inelastic cross section has been derived from accelerator data on p-p and $\bar{p}$-p collisions, up to $E_{lab} \sim 10^5$GeV. At still higher energies there are air shower results from Akeno (Hara et al. 1983 and conference paper EA3-14) and the Fly's Eye (Cassiday et al.

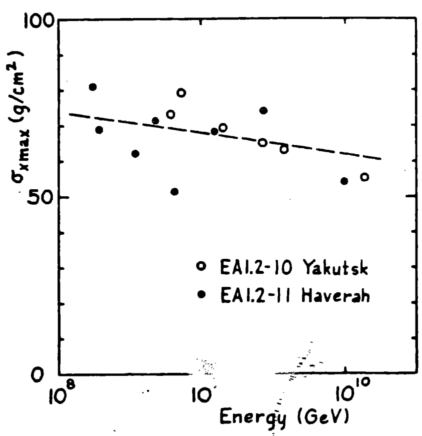

Fig. 12. Dispersion of the elongation, x_{max}, vs primary energy.

1982). For the present purpose I will adopt an expression which is consistent with everything one knows up to $\sim 10^{10}$GeV:

$$\text{cross section}\Big|_{\text{p-air}}^{\text{inel.}} \text{(mb)} = 270 + 3.3 \log^2 E \text{ (GeV)} .$$

Assuming constant composition, as I have done, the tendency for σ_{xmax} to decrease with increasing energy as shown by Fig. 12 results from the energy dependence of the interaction cross section. For consistency with the formula just given the slope should be ~ 6 g/cm^2 per decade, somewhat less than the experimental best value but within the errors. (If one assumes that <a> decreases somewhat in this broad interval then of course the fit is improved. See Fig. 18.)

Figure 13 shows the result given by Eq. 7 for $E = 10^9$GeV. The results for 10^8 and 10^{10}GeV are similar. The two quantities which it is feasible to measure at air shower energies, <a> and σ_a, are plotted as rectangular coordinates. For any pure composition $\sigma_a = 0$. It is assumed that the possibilities range from a = 0 (pure protons) to a = 4 (pure Fe). The maximum σ_a for a given <a> occurs for a mixture of protons and Fe nuclei. When the scales are chosen as I have done, the locus of binary proton-Fe mixtures is a semicircle. The dash lines correspond to ±10% errors in the most probable value of σ_{xmax}. All compositions within the shaded area are about equally probable according to these data. Although most of the semicircular area lies outside the shaded region, the range of compositions (<a>, σ_a) that are allowed by these data is very wide. It includes, alas, every composition listed in Table 1 except one out-dated result at 10^4GeV. Nevertheless, by drawing additional curves corresponding to greater and greater deviations from the best curve it can be shown that a composition consisting almost entirely of Fe, or any composition lacking a significant proportion of protons or alpha particles, can be ruled out with very high confidence.

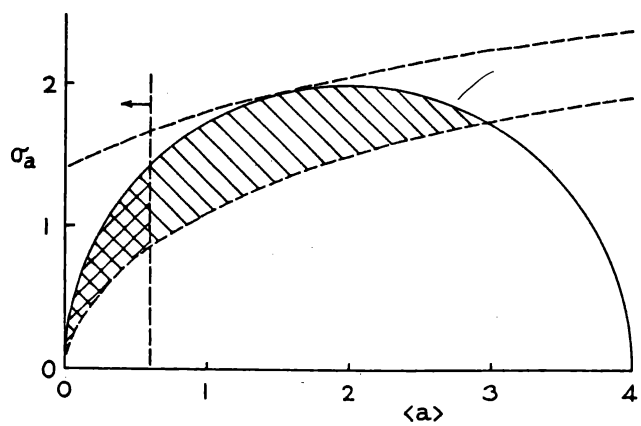

Fig. 13. Logarithmic primary mass dispersion vs logarithmic average primary mass. Possible compositions, assuming that primaries are nuclei no heavier than Fe, are those inside the semicircle. The shaded region is allowed according to results on σ_{xmax} (dashed boundaries correspond to ± 1 std. dev.) The crosshatched region is allowed according to these results and also results on $<x_{max}>$.

3.3 Energy dependence of xmax. Another method of investigating composition in the air shower domain uses data on the *average value* of an observable having the same property, that its graph vs logE is a straight line. By superposition one finds that

$$<y> = y_0 + b(\ln E - <a>) \quad . \tag{9}$$

4

The trouble is that the constant term y_o is model dependent.

This method has also been applied to data on x_{max}. There are strong theoretical arguments that in this case the rate parameter is equal to the radiation length (37.1 g/cm^2 in air) minus a reasonably small correction whose model dependence is well understood (Linsley and Watson 1981, Cherry et al. 1983, Hein and Kanevsky in paper EA2-20 of this conference). According to (9), an observed elongation rate which differs markedly from the theoretical value is a signature of changing primary composition.

Evidence reported a few years ago indicated in this way that the value of $<a>$ undergoes a drastic decrease, $\Delta<a> \sim -4$, in the interval 10^6-10^8GeV (Thornton and Clay 1979). In this experiment x_{max} was derived from time profiles of atmospheric Cerenkov light observed at sea level. High altitude counter experiments also indicate that x_{max} is unexpectedly small at the lower end of this energy range (Antonov et al. conference paper EA1.1-14 and references therein), but the precision is not very great. After reviewing the data that were available up to the time of the previous conference Watson and I concluded that there was good evidence for the fact of a change, but the magnitude of the change was not required to be so great; $\Delta<a> \sim -1.5$ was sufficient to explain the data, allowing for the errors (Linsley and Watson 1981). Results reported since then are consistent with this conclusion.

Alternatively one can try to evaluate the term y_o in Eq. 9, as well as b. Watson and I did this, using accelerator-based evidence on x_{max} for proton showers up to 10^2GeV and extrapolating on the assumption that scaling is violated no more than the accelerator evidence requires. We described our result in terms of a mixture of 'normal' material with $<a> = 1.5$ and additional protons. Restated in terms of the over-all average, our conclusion was that above $3\cdot10^7$GeV, $0 < <a> < 0.6$ (2 standard deviation upper limit). This result is also shown in Figure 13.

3.4 Application to muon data. Another air shower observable to which these considerations apply is $\ln N_\mu$ where N_μ is the muon size. As I explain in the Appendix, because N_μ is a type-F observable (using terminology due to Peters), proportional that is to A for primaries with a given energy per nucleon, whereas x_{max} is a type-G observable, independent of A, Eq. 9 must be changed to

$$<y> = y_o + b\cdot \ln E + (1-b)<a> , \qquad (10)$$

where, as before, $b = dy/d(\ln E)$. For $y = \ln N_\mu$ the derivative is < 1, so the order of lines in the mass spectrum is reversed: protons $\rightarrow$ Fe for increasing $\ln N_\mu$ as against Fe $\rightarrow$ protons for increasing x_{max}. In Eq. 7, b must be replaced by (1-b). The fact that most of the measurements are of N_μ for a given electron size N_e rather than a given energy makes no essential difference: Eq's 7-9 can still be used, lnE being replaced by $\ln N_e$ with a corresponding re-interpretation of σ_1. A practical consequence is that in general σ_1 will be a good deal larger.

3.5 Energy dependence of average Nμ. It was recognized early on that a primary composition change, such as will occur for example when mixed-composition cosmic rays undergo a rigidity cutoff, ought to be revealed in air shower data by a change in $d(\log N_\mu)/d(\log N_e)$ (Peters 1960, De Beer et al. 1968). If one proceeds in the same manner as with x_{max} one can conclude from data above 10^8GeV, where the composition appears to be constant, that in this case (1-b) = 0.23 ± .03. According to (10), if the average primary mass indeed decreases in the interval 10^6-10^8GeV by the amounts discussed above (Δ<a> = -1.5 to -4), then $d(\log N_\mu)/d(\log N_e)$ ought to dip, in this interval, to values 10 to 30% lower than normal. Evidence for a 10% dip in about this region was pointed out by Catz et al. (1969) in results from Verriéres. The muon energy threshold was not given; presumably it was 5 GeV or less. Results for similar thresholds compiled by Khristiansen et al. (1980) do not confirm this dip. The strongest contradiction to the Verriéres result is by the one from Tien Shan (E_μ > 5 GeV) reported by Danilova et al. (1981), extending from < 10^5 to > 10^7GeV with good statistical accuracy. The Tien Shan result has been interpreted to mean that there is no significant change in primary <a> over that energy interval. This of course conflicts with the conclusions drawn from the evidence on x_{max}. Proponents of constant <a> argue that the enhanced elongation rate results from a change in particle physics, not composition; proponents of a decrease in <a> argue that the effect of changing composition on N_μ is masked by a compensating change in particle physics. Most authors agree, however, that of the two, x_{max} is less model-sensitive than N_μ.

The model-sensitivity of N_μ calculations can be decreased by increasing the muon energy threshold. At this conference the results shown in Figure 14 are presented by the Kolar group (paper OG4-8 by Acharya et al.). The muon energy threshold is 220 GeV. The results are in good agreement with a reduction in <a> by 1.5 in 2 decades, beginning ∿ $3 \cdot 10^6$GeV. It is noteworthy that the size spectrum given by the same experiment has no change of slope in the region where $d(\log N_\mu)/d(\log N_e)$ is seen to change. The size spectrum does show a kink but it occurs at a higher primary energy. The discontinuity in $d(\log N_\mu)/d(\log N_e)$ corresponds to the energy at which the slope of the all-particle spectrum changes most rapidly (Acharya et al. 1981 and paper OG4-8; see Fig. 11 above).

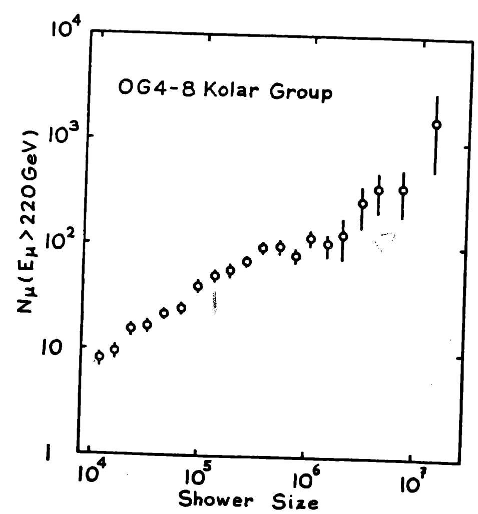

Fig. 14. Average number of high energy muons vs shower size at Kolar.

As in case of x_{max} one can attempt to determine <a> itself from the N_μ data by evaluating y_o in Eq. 10. Although as I remarked above there is generally more uncertainty about calculating N_μ, here the circumstances are relatively favorable: 1) the muon energy is high enough so that it is unnecessary to track the cascade process through many generations, and 2) the primary energy is not extremely high, so it is not necessary to extrapolate very far beyond the accelerator region.

6 Ref. + App.

On the basis of their calculations these authors find good agreement below $3\cdot10^{6}$GeV with a 'normal mixed composition', which they define as the composition measured at 10^{3}GeV (<a> = 1.5). They express great confidence that <a> cannot be as great as 4 (pure Fe) in this region.

3.6 Fluctuations in $N\mu$. Muon data are also used to estimate σ_a (Linsley and Scarsi 1962, Dzikowski et al. 1977, Stamenov et al. conference papers OG4-11 and 12, Hara et al. paper EA1.2-14). With reference to Eq. 7, the value to be used for b in the interval 10^{6}-10^{8}GeV is somewhat uncertain in view of the conflicting interpretations of the average data. If there is a changing composition in that interval such that Δ<a> = -1.5 then the value of b (which characterizes *proton* showers) must be $\sim$ 10% higher than $d(\log N_\mu)/d(\log N_e)$ so as to compensate. However the main uncertainties are in σ_1 and k, which cannot be measured and therefore must be calculated by the Monte Carlo method using a particle physics model. The fluctuations which must be taken into account are mainly those in N_e with respect to E, the primary energy. These go through a minimum at about the level of maximum development, which in practice is always higher than the observation level. They are expected to increase steadily with increasing depth past x_{max}. The minimum value of σ_1 is thought to be 0.15-0.20. At 200 g/cm^2 past maximum it may be 0.30-0.35; at 300 g/cm^2 past, it may be 0.5 (Linsley 1963, 1967; De Beer et al. 1968; Elbert et al. 1976).

The observed spectra (frequency distributions of $\log N_\mu$ or sometimes N_μ itself, for fixed N_e) are entirely featureless. Figure 15 shows an example. The dispersion σ_y decreases steadily as N_e increases, becoming $\sim$ 0.3 at 900 g/cm^2 depth for $N_e = 10^8$ (Hara et al. paper EA1.2-14; see also Efimov et al. paper EA3-15). A dispersion this small is incompatible with a primary mass spectrum as broad as at 10^{3}GeV (where $\sigma_a \sim 1.5$; see Table 1). Three results obtained using Eq. 7 are shown in Figure 16. In this case the terms

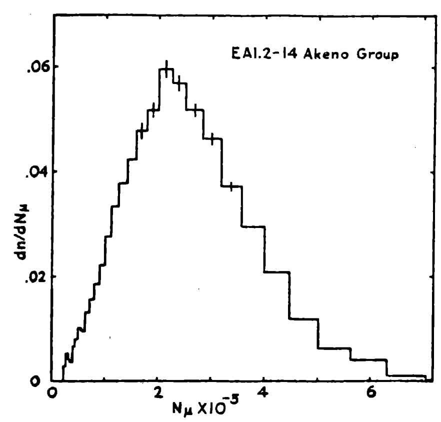

Fig. 15. N_μ *spectrum for fixed electron size* ($\log N_e = 6.8$) *at Akeno.*

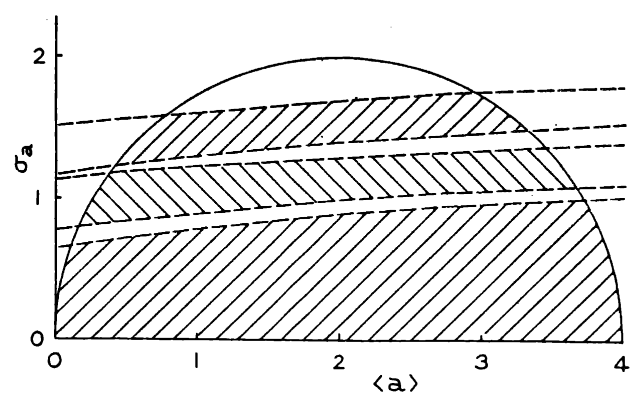

Fig. 16. Logarithmic primary mass dispersion vs logarithmic average primary mass. The upper shaded region is allowed, at E $\sim 3\cdot10^{6}$*GeV, according to results at Tien Shan on the width of the* N_μ *spectrum for fixed* N_e*. The middle and lower regions are allowed, at E* $\sim 10^{8}$*GeV, according to similar results at Akeno and Volcano Ranch, respectively.*

involving <a> are relatively unimportant; a fairly good approximation is given by $\sigma_a^2 = (\sigma_y^2 - \sigma_1^2)/(1-b)^2$. In all cases I have assumed k = 0.15, b = 0.77. For Tien Shan I used $\sigma_y = 0.40 \pm .03$ (Nikolskii et al. 1979), $\sigma_1 = 0.25$; for Akeno, $\sigma_y = 0.30 \pm .03$, $\sigma_1 = 0.20$; for Volcano Ranch, $\sigma_y = 0.15^{+.10}_{-.05}$ (after subtraction of the instrumental dispersion), $\sigma_1 = 0.20$. The latter two results apply to primary energies 10^8-10^9GeV; the former result, to 10^6-10^7GeV. It is notable in this case, as in the previous one using x_{max}, that *measurements of spectral width* (so-called 'fluctuations') *are less effective at providing constraints on composition models than are measurements of spectral location* (average line location). The primary mass dispersion observed at Tien Shan is the same as given in Table 1 for 10^3-10^4GeV. At the higher energies the dispersion is less; the composition is more nearly pure. There is good consistency with the x_{max} results shown in Fig. 13.

Some primary composition tests can be applied to the very largest air showers. For example one may know the muon content as well as E_{EM}, or one may have an estimate of x_{max} from the signal risetimes. These tests indicate that the highest energy primaries — say those above the ankle, or even those few with E > 10^{11}GeV — are not radically different from those I have been discussing. They are not dust grains, they are not neutrinos, they are not magnetic monopoles, quark globs or mini-black holes.

3.7 Other methods. High energy hadrons and γ-ray families, and very high energy (> TeV) muons, also provide information that is important for disentangling the effects of primary composition and particle physics. At present experiments on these components are limited to energies < 10^7GeV. By and large the hadron evidence is described as favoring a 'normal' composition in the 10^6-10^7GeV region (see Erlykin and Kuzina 1981, Wdowczyk and Wolfendale conference paper EA3-23). Interpretations of such evidence as favoring a primary composition enriched in heavy nuclei (Amenomori et al. papers HE5-17 and 18, Mincer et al. paper OG4-10) are disputed by other authors (Kempa and Wdowczyk paper HE4-33, Sreekantan et al. paper EA1.1-50). The possibility of a modest proton enrichment in this region such as I propose here (Part 4) has not been considered. I believe it will be found consistent with the hadron evidence and with the closely related evidence from γ-ray families (see Krys et al. 1981).

A by-product of the proton decay experiments is a keen new interest in deriving results on the primary composition from measurements of multiple muons deep underground. Unless the accompanying air showers are measured the character of the cosmic ray sample is difficult to describe; it is neither fixed energy per nucleon nor fixed energy per particle. Hence comparisons are made by means of simulations. An early result from the Utah group favors a so-called 'low energy composition' like the Ellsworth et al. model in Table 1 (<a> = 1.1); a more recent one from the Homestake experiment (Cherry et al. 1981) favors a model with more heavy nuclei (Elbert 1982). At this conference preliminary data from the NUSEX experiment are similarly compared (Battistoni et al. paper HE7.2-7). In all these cases the primary energy is ∿ 10^6GeV.

4. MODELLING THE HIGHEST ENERGY COSMIC RAYS

I will use the term 'population' to denote a group of cosmic rays with the same source composition which are accelerated and propagate under the same average conditions. In this sense particles accelerated in solar flares are a different population than galactic cosmic rays. One wishes, of course, to explain all cosmic rays in terms of a minimum number of populations. Even in case of different populations, one wishes to minimize the difference by assuming, for example, that the source composition is the same, the acceleration mechanism is the same, or the like (J. P. Meyer 1983 and conference paper OG6-37).

Nearly all of the observed features of cosmic rays below 10^3GeV (excluding solar cosmic rays) are accounted for as properties of a single population. The apparent over-abundance of antiprotons is exceptional. An attempt made by Colgate (1975) to account for the entire all-particle spectrum by extrapolating the low-energy properties, assuming direct acceleration by type I supernovae, requires special assumptions in order to explain the anisotropy of the highest-energy particles (Colgate, conference paper OG6-4). But if the knee is explained by a simple rigidity cutoff, as in this proposal, the average primary mass begins to *increase* at the knee, the value of $\langle a \rangle$ approaching 2.7-2.8 rather than decreasing to < 0.6. A cutoff (change of exponent) abrupt enough to account for the knee, acting on the sort of composition found at 10^2-10^3GeV, would produce a characteristic 'transition region' about 1.5 decades wide, which is not present (Hillas 1979, 1983). Finally, the all-particle intensity is higher, in the region 10^5-10^7GeV, than one can account for by an extrapolation based on the observed power law exponents of individual primary elements. The principle that all primary nuclei have the same rigidity spectra, which seems to apply quite accurately up to 10^3-10^4GeV, is evidently violated in the region of the knee. If the knee belongs to the low energy population, then one must look to some loss mechanism whose threshold for different nuclei is at about the same energy per particle rather than the same energy per nucleon.

The possibility of explaining the knee along these lines was pointed out as early as 1963 by Zatsepin et al. A specific mechanism, photodisintegration in the source region, has been discussed by Hillas (1979). A phenomenological model incorporating these ideas has been proposed by Nikolskii (1975 and conference papers OG4-12, 14). According to his model both $\langle a \rangle$ and σ_a remain practically constant above 10^3-10^4GeV.

Alternatively the knee may belong to a different population. In the closed galaxy model of Peters and Westergaard (1977) there are two populations, young and old. The equal-energy composition changes in a complicated way: Fe predominates at 10^5GeV, protons and alphas are predominant at 10^7GeV (the knee energy), while at higher energies the average mass again increases. This behavior is contrary to the evidence; furthermore the model predicts too small an anisotropy at the highest energies.

The local superbubble model of Streitmatter et al. also assumes two populations, one from interior and the other from exterior sources (conference paper OG5.1-9). As in case of the Peters-Westergaard model the two populations are assumed to originate in the same manner, differing only in regard to propagation. With the usual assumptions about source spectra (Shapiro-Silberberg abundances, equal-exponent power laws for the spectra of primary elements) the different low energy spectra of primary and secondary elements observed near the earth are explained. There is a rather gradual rigidity-dependent steepening of the various interior spectra due to outward leakage. At high enough energies the exterior population leaks inward and eventually becomes dominant. The shape of the all-particle spectrum can be adjusted to fit the observations by means of parameters which describe the leakage. The anisotropy is explained at least qualitatively. However in the versions described to date, in which the exterior population has about the same value of <a> as the interior one, the average mass of the observed mixture undergoes a strong increase beginning at an energy where the superbubble wall starts being transparent to protons and ending about where the flux of exterior protons equals the flux of interior Fe nuclei. After this increase <a> relaxes to about the low energy value. This behavior is of course contrary to the evidence from air shower experiments.

A two-population model of another type, assuming a pulsar origin of the 10^5-10^{10}GeV cosmic rays, is described in conference paper OG6-22 by Silberberg et al. Three of the four variants predict a composition enriched in heavy nuclei at 10^8GeV, contrary to observation. The remaining variant (1) invokes the Hillas mechanism (photonuclear interactions) to explain the knee. It predicts a relatively high flux of $> 10^5$GeV neutrinos, observable with a DUMAND-type detector. The acceleration mechanism, taken from work by Michel and Dessler (1981), does not restrict the composition of the material that is accelerated. However Berezinskii (1983) concludes that cosmic rays accelerated by pulsars are likely to be alpha particles. In an earlier pulsar model due to Karakula et al. (1974) the acceleration process was limited to proton energies $< 10^8$GeV (Fe energies $< 3 \cdot 10^9$GeV).

A phenomenological model which correctly describes the composition evidence at all energies as well as the all-particle spectrum is shown in Figure 17. In addition to the low energy population there is a high energy population consisting entirely of protons. This population becomes dominant above $\sim 10^6$GeV; the knee belongs to it. It is immaterial whether one assumes the knee to be as abrupt as I have shown it here or a good deal more gradual. I have not tried to separate the over-all proton component into two constituent parts because, again, the evidence allows a good deal of latitude about how this can be done. As Fig. 1 shows, the assumed flattening of the over-all proton spectrum does not conflict with balloon results in view of the large errors. Evidence in favor of such a flattening is given by the high precision muon measurements of Klemke et al. (1981). The low energy population is assumed to have a rigidity cutoff, but the transition region is not visible because where it occurs the high energy population has already become dominant. Quantitatively the model is given by

$$j_i(E)dE = W_i(E/E_i)^{-\gamma}dE \quad , \qquad (11)$$

for i = 2 to 5, where j is the differential flux in $m^{-2}sr^{-1}s^{-1}GeV^{-1}$,

$$E_i(\mathrm{GeV}) = 5 \cdot 10^5 \langle Z \rangle_i \quad , \qquad (12)$$

and
$$\gamma = \begin{cases} 2.73 & \text{for} \quad 0.01E_i < E < E_i \\ 3.23 & \text{"} \quad E_i < E \end{cases} \quad (13)$$

The proton flux (i = 1) is taken simply as the difference between the observed all-particle flux and the flux of heavies according to (11), summed for i = 2 to 5. The fraction of protons decreases from about 55% at 10^2GeV to 35% at 10^3-10^4GeV and then increases smoothly, reaching 75% at 10^7GeV and 92% at 10^9GeV. Values of W for the heavy nuclei are given in Table 5.

Table 5. Values of the parameter W

index i =	2	3	4	5
element or group	He	CNO	Z=10-20	Z=21-26
<Z>	2	7	14	26
<A>	4	14.5	24	56
W ($m^{-2}sr^{-1}s^{-1}GeV^{-1}$)	3.4×10^{-13}	7.7×10^{-15}	1.5×10^{-15}	2.4×10^{-16}

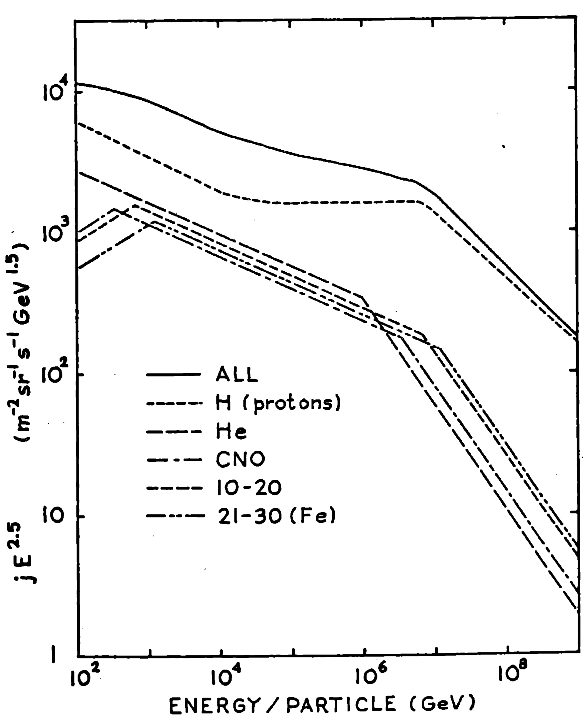

Fig. 17. Observed all-particle spectrum (solid line) and phenomenological spectra for various charge groups constructed so as to be consistent with it.

They were chosen to fit the low energy data at 10^4GeV. Values of <a> and σ_a given by the model are shown in Figure 18 together with the experimental results discussed in Parts 1 and 3. There is good agreement with all of the air shower evidence.

Note that as the energy increases the value of σ_a does not drop below 1 (half of the greatest value it can possibly have) until <a> has fallen to 0.6 and the fraction of protons has climbed above 90%. But combinations like $\sigma_a \sim 1$, <a> $\sim$ 0.6 occur at low energies also. It is essential therefore to avoid using qualitative terms like 'normal composition' and 'low energy composition' to describe the results of air shower experiments: the range of ambiguity is comparable to the maximum range that can occur.

It seems not too difficult to provide an astrophysical basis

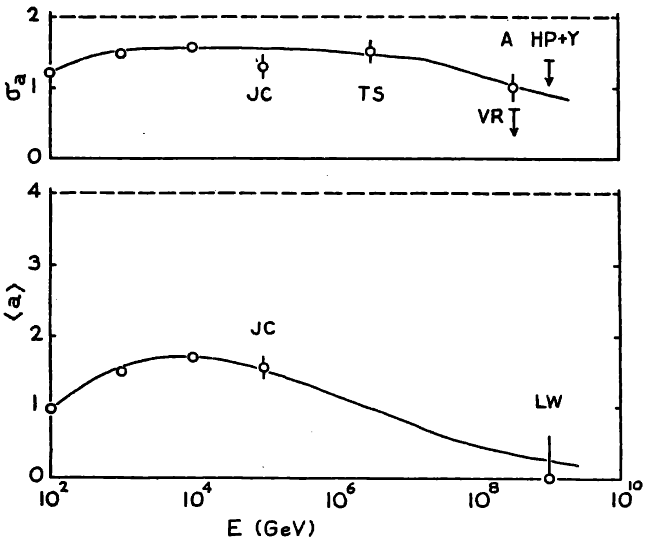

Fig. 18. Logarithmic primary mass dispersion and logarithmic average primary mass, vs energy. The 3 lowest-energy points are from Table 1. Points JC are derived from JACEE results (paper OG4-5). Points TS, A and VR are derived from N_μ fluctuation measurements at Tien Shan, Akeno and Volcano Ranch, respectively (see Fig. 16 and text). Point HP+Y is derived from x_{max} fluctuation measurements at Haverah Park and Yakutsk (see Fig. 13 and text). Point LW is from Linsley and Watson (1981).

for this sort of model. Reasons for believing that low energy cosmic rays are confined very near the solar system are summarized by Ormes in conference paper OG5.1-10. As he remarks, their source composition may be atypical, and they may have sampled in their motion an abnormally low-density portion of the galaxy. One expects the high energy population to be more nearly average in both respects. It seems clear that the superbubble model could be modified so as to agree with the high energy composition data; however it is unnecessary to postulate that specific physical barrier between populations. It appears that the pulsar model of Silberberg et al. could also be brought into agreement.

A two-population model that is similar in some respects to the superbubble model was proposed early on by Fichtel (1963). The observed low energy cosmic rays are assumed to be typical of the spiral arm segment containing the solar system, while the high energy ones are typical of the halo. He estimated that the total amount of material traversed by the halo population might be as great as 150 g/cm^2, far more than would be required to produce a sufficient degree of proton enhancement, starting with solar-type material.

In the same article Fichtel proposed interpreting the ankle of the all-particle spectrum as marking a transition from predominantly galactic to metagalactic cosmic rays, presenting reasons for expecting the transition energy to be $\sim 10^{10}$GeV. Recently this interpretation has been revived in work by Shapiro and Silberberg (1983). In conference paper OG8-2 by Schramm and Hill the blackbody cutoff mechanism is re-examined. It is pointed out that the pileup effect due to repeated collisions, which is quite small for the usual assumptions about source spectra, would become quite large in case of a source spectrum that is sufficiently hard; e.g, $1/E^2$ above $2 \cdot 10^{10}$GeV.

Other conference papers related to the problem of explaining metagalactic cosmic rays are OG6-1 by Colgate and OG8-1 by Fischhoff. Colgate shows that protons and other nuclei accelerated to very high energies by active galactic nuclei will be unable to escape without suffering disastrous losses in collisions with ambient photons. If such objects are indeed sources of the highest energy cosmic rays (Lovelace 1976, Blandford and Payne 1982, Lake and Pudritz 1983) it must be assumed that the escaping particles are neutrons from collisions deep inside (Berezinskii 1983). A suggestion that neutrons might similarly make it possible to circumvent the Greisen-Zatsepin effect was made earlier by Wdowczyk and Wolfendale (1976). Cosmic rays that have undergone this process will of course be protons.

Fischhoff describes an ingenious model in which a very small proton-electron positive excess charge (consistent with the lowest upper experimental limit), taking effect within the framework of galactic evolution, results in acceleration of cosmic rays to 10^9-10^{11}GeV. Such cosmic rays would presumably have the composition of primordial matter, a mixture of hydrogen and helium.

5. ANISOTROPY

5.1 Harmonic analysis in sidereal time: results of measurements. The Munich Conference in 1975 marked a change in viewpoint regarding cosmic ray arrival directions, an abandonment of the hypothesis-testing paradigm (can one disprove that cosmic rays are perfectly isotropic and thus 'discover' anisotropy?) and a return to the quantitative description paradigm (what limits and confidence levels can be obtained for the cosmic ray anisotropy?) Adherents of the latter viewpoint whose example set this change in motion were Sakakibara (1965) and Gombosi et al. (1975) for the lower range of air shower energies and Krasilnikov (1974) for the upper range.

Except at the highest energies the anisotropy is so small that the method of measurement must be highly sensitive. The only method having the required sensitivity makes use of the earth's rotation. Anisotropy induces periodicity in the response from a cosmic ray detector, having a fundamental frequency corresponding to the duration of a sidereal day. A periodicity of this kind, interpreted as an effect of galactic rotation (Compton and Getting 1935) was reported as early as 1933 by Hess and Steinmaurer. The principal results that have been obtained to date by this method are summarized in Figure 19.

The earliest data shown were derived by Daudin et al. (1956) from the counting rate of small air showers at mountain elevation. The amplitudes reported are so small in relation to atmospheric temperature and pressure effects that their accuracy as a measure of cosmic ray anisotropy remained in doubt for many years. Similar measurements at higher energies, where the anisotropy was expected to be greater in relation to masking effects, produced results that seemed to be contradictory.

Following a report by Krasilnikov at the 1974 European Symposium in Lodz, important steps were made toward understanding apparent contradictions in the data for very large air showers ($E > 10^8$GeV). At the same time, a new experiment on small air showers was being performed with great care by a Hungarian-Bulgarian group headed by Somogyi. The results of that work (Gombosi et al. 1975, 1977) were soon confirmed very accurately by work done at Norikura (Sakakibara et al. 1976, 1979). Additional confirmation has

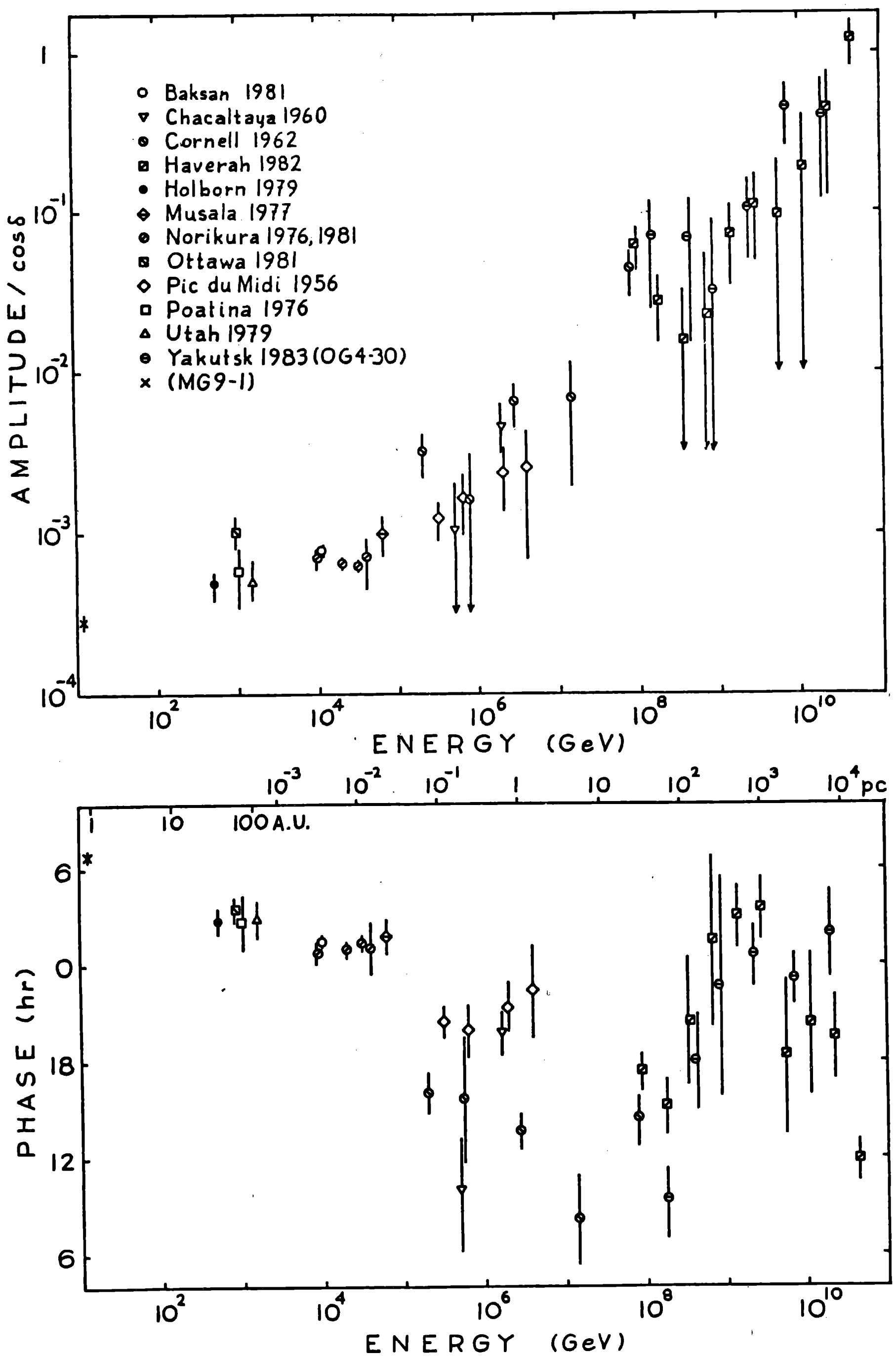

Fig. 19. *Cosmic ray anisotropy from harmonic analysis of counting rates in sidereal time. Shown above are the equatorial projected amplitude and phase of the first harmonic (δ being the latitude of the experiment). On the following page are the corresponding results for the second harmonic.*

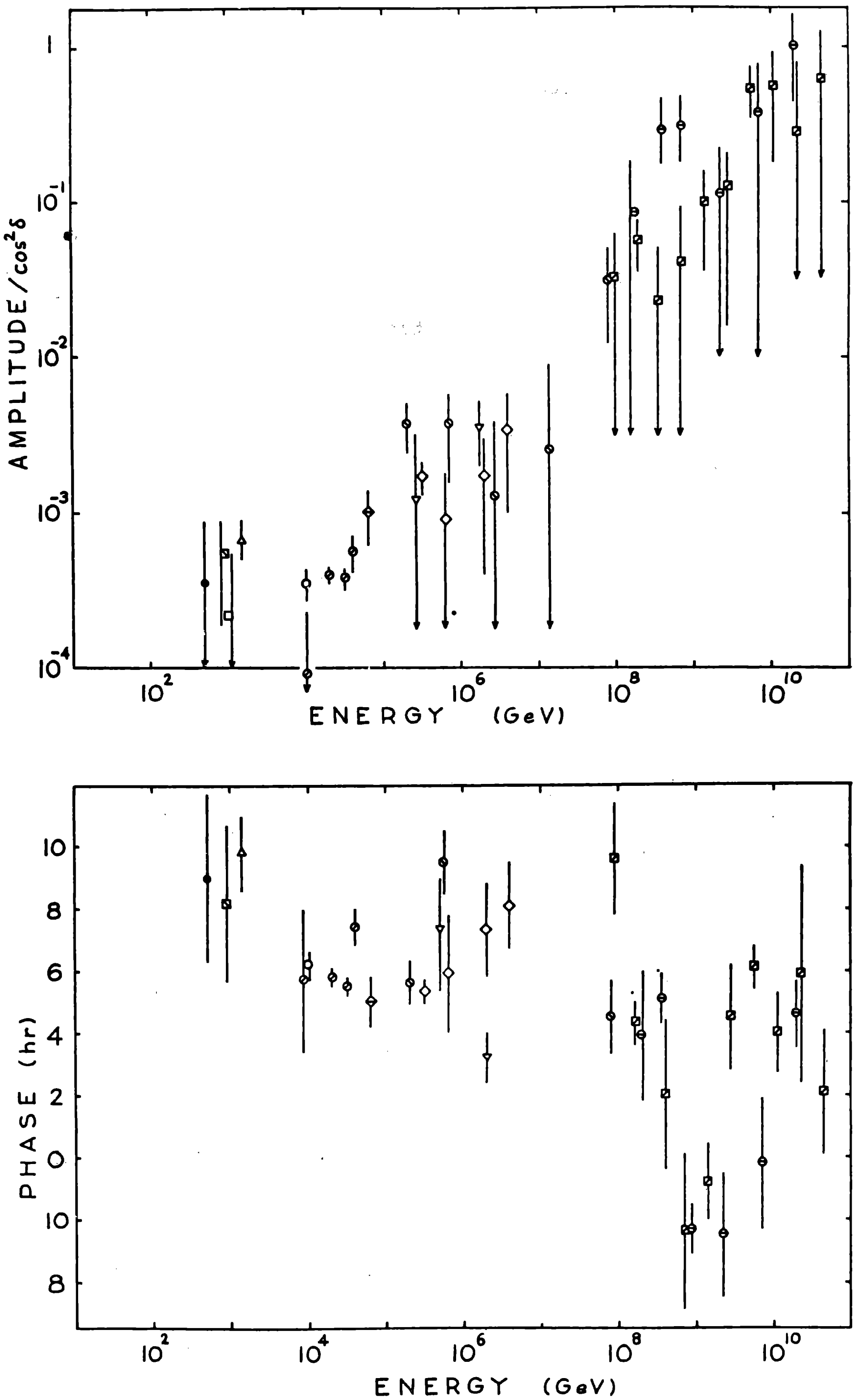

AMPLITUDE / $\cos^2\delta$
1
10^{-1}
10^{-2}
10^{-3}
10^{-4}
10^2
10^6
10^8
10^{10}
ENERGY (GeV)
PHASE (hr)
10
8
6
4
2
0
10
8
10^2
10^4
10^6
10^8
10^{10}
ENERGY (GeV)

been provided by results of the Baksan experiment (Alexeenko et al. 1981). There is good consistency between this group of results for 10^4-10^5GeV and a group at $\sim 10^3$GeV derived from experiments with underground muon telescopes (Fenton and Fenton 1976, Davies et al. 1979, Bergeson et al. 1979, Berkovitch and Agrawal 1981).

Using the results on small air showers as a basis I will proceed to discuss the remaining evidence. I will argue that within the error estimates, as given by the various authors, all of the data in Fig. 19 should be accepted without any reservations about spurious effects of a statistical, instrumental or atmospheric nature, but with two understandings: 1) that for energies < 10^9GeV the primary energy resolution is poor, and 2) that below 10^9GeV the energy calibrations are often uncertain by something like a factor of 2.

The success of the small shower experiments shows that the residual effect of instrumental instabilities can be held to 1 part in 10^4. At the higher energies it would take outrageously large instabilities to have a noticeable effect. One can also conclude that atmospheric effects are less worrisome than they were sometimes feared to be. The fact that such good agreement was obtained at Baksan is especially impressive because the data were for a single year, corrected only for atmospheric pressure variations. The question of a possible selection effect favoring large apparent anisotropies (Greisen's despairing suggestion that "below this line [drawn at a level equal to twice the expected rms accidental amplitude for random fluctuations] belong an enormous number of ... unreported points" - Delvaille et al. 1960) was dealt with by noting that in fact all significant efforts in this field *have* been reported in the literature. It was shown that when all of the results are combined, using proper statistical weights, no such selection effect is seen, and the combined results cannot be explained by random fluctuations (Linsley and Watson 1977). Instead of showing the well-known combined points here, I show the results of 3 individual pre-1965 experiments which differed from all the rest in that the counting rates were corrected for atmospheric pressure variations (Daudin et al. 1956, Escobar et al. 1960 and Delvaille 1962). These experiments cover the range 10^5-10^8GeV with statistical accuracy which has not been improved upon since they were done. Above 10^8GeV one can now add to the data from Haverah Park (Lloyd-Evans and Watson 1983, Lloyd-Evans 1982) new results from the Yakutsk experiment (Efimov et al. conference paper OG4-30). The six Yakutsk points are based on 14,000 showers of which 115 had E > 10^{10}GeV. The ten Haverah points are based on 90,000 events.

Looking at the 4 parts of Fig. 19 from the viewpoint I am suggesting, one can ask, what are these data trying to tell us? Clearly, that

1) There are significant first and second harmonics over the entire energy range.

2) There is a general tendency for the amplitudes r_1 and r_2 to increase with increasing energy. Note that on the basis of Davis's theory for relating cosmic ray anisotropy to harmonic amplitudes I have divided r_1 by $\cos\delta$ and r_2 by $\cos^2\delta$ where δ is the latitude of the experiment (Davis 1954).

3) Below 10^5GeV the first harmonic is not as constant as it once seemed to be; certainly the phase varies. The second harmonic also seems to be energy dependent in this interval as well as at higher energies. Note that just to see how it would look, I have included a very low energy result reported at this conference by Nagashima et al., derived from a mammoth collection of neutron monitor records (paper MG9-1). The energy assigned to this point is my own guess.

4) Both the first and second harmonics show dramatic changes in phase. It may be recalled that in 1965 Sakakibara pointed out that the early air shower data favored a change in the first harmonic phase from about 20 hr below the energy of the knee to about 12 hr above it. When Watson and I took into account the relative statistical weights of these results we found that they favor a more or less linear decrease with increasing logE. Our best straight line agrees well at lower energies with the Musala result and agrees well at higher energies with results from Haverah. Within a few years the next meander in the first harmonic phase could be made out: I mean the rapid increase from $\sim$ 12 hr at 10^8GeV to $\sim$ 24 hr at 10^9GeV, followed by an almost equally rapid decline. This behavior in the region 10^8-10^{11}GeV has now been seen in results from all 3 giant arrays in the northern hemisphere: Haverah Park, Volcano Ranch (Linsley 1975) and Yakutsk.

At the energies observed with these arrays the argument for using harmonic analysis in sidereal time loses some of its force. On the one hand are technical considerations: harmonic analysis is effective for revealing broad directional features in large samples of events measured with poor angular resolution but good stability. Here the samples are not very large but the angular resolution is good, both in right ascension and in declination. On the other hand, astrophysical considerations favor use of galactic coordinates and methods better suited for describing small-scale clumps and clusters. Nevertheless, even above 10^8GeV results of harmonic analysis in right ascension provide a useful test of consistency when applied, as they are here, to experiments covering more or less the same declination band.

In the presence of such large, rapid changes of phase it is obviously essential to have rather good energy resolution and to divide one's data into rather narrow energy bins; otherwise amplitudes are liable to be under-estimated. Note that at energies just below 10^9GeV, and again at energies $\sim 10^{10}$GeV, where the first harmonic phase is changing most rapidly, measurements of the first harmonic amplitude are barely out of the noise, as shown by the fact that the experimental points have large error bars and in some cases give only upper limits. This is expected as a result of destructive interference, due to the limited energy resolution and the necessity of using factor-of-2 energy bins in order to have adequate numbers per bin.

5) It is by no means established that the amplitude increases are smooth and gradual. There is fairly strong evidence, in fact, for a feature in r_1 vs E at $\sim 10^8$GeV. The Leeds group has agonized at great length over the question of whether the apparent peak here is real or not, concluding that

due to certain ambiguities in the over-all evidence it cannot yet be claimed as a discovery (Lloyd-Evans and Watson 1983). One can comment, however, that these ambiguities, which are reminiscent of those which drove Greisen and his co-workers almost to despair, can also be explained as *consequences* of such a peak, if one is willing to grant that the different experiments to be compared have slightly different energy calibrations, and that there may have been a slight glitch in the Haverah energy calibration, associated with a change in the trigger condition, in March 1971. Be that as it may, the two lowest-energy Haverah points in Fig. 19 are the results obtained *before* correction on the basis of an observed antisidereal wave. I disapprove of such corrections. Thus these points differ slightly from the 'best values' given by Lloyd-Evans et al. (1982). There is also a suggestion of a peak just above 10^5GeV. In case of r_2, there seems to be a very rapid rise beginning $\sim 3\cdot10^4$GeV followed by a 'shoulder' from 10^5 to 10^7GeV after which there is another rapid rise.

5.2 Interpretation of sidereal time variations. It may be that none of these features is real; that in fact r_1 and r_2 simply increase smoothly above 10^4GeV, more or less as $\sqrt{E}$. It may be also that the phase exhibits only broad features like the 'big bend' in ψ_1 above 10^8GeV. On the other hand, I know of no compelling argument against a proposal that all of these variables (r_1, r_2, ψ_1, ψ_2) may depend on E in a quite complicated manner above 10^4GeV.

In the plot of ψ_1 vs E a distance scale is shown, with values ranging from 1 astronomical unit to 10^4parsec. These distances are Larmor radii corresponding to the energies on the lower scale, assuming singly charged cosmic rays and a uniform magnetic field intensity of $3\cdot10^{-6}$Gauss. The conventional picture in which cosmic ray propagation is described by simple diffusion is attractive, but as the galaxy is seen using EM radiation of various wavelengths it exhibits clearly delineated structure with a wide range of scale lengths. If we assume that the galactic magnetic field is organized into cells and sub-cells according to some hierarchy, or just that there are 'clouds' and 'cloudlets' as discussed by Bell et al. (1974), it seems that the suggested amount and type of energy dependence in these harmonic components could be quite well accounted for. Be that as it may, in order to have the sort of phase changes that are undoubtedly present in case of the first harmonic it seems that one must have cosmic ray streams that interpenetrate each other. This picture immediately suggests the likelihood of enhanced anisotropy (increased amplitude) if the directions of flow are the same, or a diminished effect if the flow is in opposite directions, at a given energy. At a different energy there will be streams belonging to a different rank in the hierarchy. If there is any substance in these conjectures it would follow that even in the 10^5-10^9GeV range, not to speak of energies which are still higher, the cosmic ray anisotropy contains a good deal more astrophysical information than has been supposed heretofore.

Although no connection is necessary, one would be pleased to find some kind of correlation between the variations in anisotropy and features of the all-particle spectrum (see Sakakibara 1965, Hillas and Ouldridge 1975, Hillas 1982). One finds very little, however. The $\sqrt{E}$ trend in r_1 begins well in advance of the knee, and the big bend in ψ_1, well in advance of the ankle.

In the low energy region ($E < 10^5$GeV) the sidereal anisotropy is used as a standard signal in studies of modulation by magnetic fields in the heliosphere (Cini-Castagnoli et al. 1975, Nagashima et al. conference paper MG9-2). One can also derive streaming directions, which presumably are associated with the direction of the interstellar magnetic field in the neighborhood of the solar system, averaged over scale lengths appropriate to the cosmic ray rigidity (see Wolfendale 1977, Kiraly et al. 1979). Finally one can relate the observations to specific mechanisms, for example the pitch-angle scattering ideas of Jokipii (1966) or the loss-cone model of Fujii (1971). When this is done the likely connection to narrow-angle anisotropies observed by Allkofer et al. (1981) should be kept in mind.

Even the present crude results on the high energy anisotropy severely constrain models of the origin and propagation of galactic cosmic rays. One can rule out, for example, models proposed by McIvor (1977), Bell et al. (1974) and Owens and Jokipii (1977, one version), as well as the Peters & Westergaard model mentioned previously (see Linsley 1981). It is easily shown that a leaky box picture with uniformly distributed sources predicts a galactic anisotropy whose magnitude increases with energy at about the observed rate (Hillas 1982). The additional problem of accounting for the *direction* of the anisotropy has been confronted only by Streitmatter et al. (conference paper OG5.1-9).

5.3 Technical demands. Only a few of the results shown in Fig. 19 have a signal to noise ratio as good as 10; all of these are below 10^5GeV. It will be no easy task to obtain data of this accuracy at higher energies. If it turns out that the anisotropy changes smoothly in the next few energy decades above 10^5GeV then perhaps one can simply extend the models now being developed to explain the lower energy data. If future experiments show that for 10^5-10^8GeV the pattern is complex then new ideas may be needed. Perhaps one could proceed stepwise, interpreting rapid changes in anisotropy in terms of boundaries between domains inside of which the magnetic field is considered constant.

It is clear from Fig. 19 that further investigation of the 10^5-10^8GeV region requires improved energy resolution as well as continually larger sensitive areas to compensate for the rapidly falling intensity. A way to achieve the required resolution is to use N_μ for the ground parameter instead of N_e. This has been done by the Akeno group (Hara et al. conference paper OG4-23). Results are given for unselected showers and also for events selected according to muon content; that is, for primaries enriched in heavy nuclei (μ-rich showers) or enriched in γ-rays (μ-poor showers). The numbers of events are still far too small to provide new information about the anisotropy of unselected primaries. An upper bound of about 3% can be set on the first harmonic sidereal amplitude of μ-rich showers. This is much lower than the amplitude found in an earlier experiment. The corresponding bound for μ-poor showers is about 5%.

5.4 Results from the southern hemisphere, and from Fly's Eye. At energies below $\sim 10^8$GeV (Larmor radii < 30 pc according to the assumptions given earlier) one expects about the same results from cosmic ray observations in the northern and southern hemispheres, after allowing in the usual way for dependence of sidereal amplitudes on $\cos\delta$. At higher energies this is not the case, so results from the SUGAR array (Horton et al. conference paper OG4-32) require separate consideration. Only the events with nominal energy > 10^{10} GeV (and zenith angle < 60°) are described; they number 140. On the calorimetric energy scale used for binning the Haverah and Yakutsk events these nominal energies are too small by about a factor of 2. Results of harmonic analysis are given for 3 declination bins. For comparison with results in the northern hemisphere I have combined them. On a common scale the average energy corresponds to Haverah bin 10, the highest-energy point in Fig. 19. The projected first harmonic amplitude is smaller and much less significant (0.18 ± .15 at δ = 34°S vs 1.2 ± .4 at 54°N); the projected second harmonic amplitude has about the same magnitude but much greater significance (0.44 ± .18 vs 0.6 ± .7).

In addition to the 1960 results of Escobar et al. plotted in Fig. 19, work at Chacaltaya has produced a substantial amount of data on larger showers (Anda et al. 1981, Aguirre 1982). The site is valuable not only for its high elevation but also for its location just south of the equator. The more recent anisotropy results are not shown here because in the light of new conclusions reached in Part 2 concerning calibration it appears that the 'new Chacaltaya' energy scale needs to be adjusted. Also the events need to be sorted into bins no wider than a factor of 2. To the extent that comparisons can already be made, the new Chacaltaya results are in satisfactory agreement with those from the northern hemisphere and those from the SUGAR experiment.

Preliminary results from the Fly's Eye experiment are given by Cady et al. in conference paper OG4-31. They indicate that possible systematic errors due to the unique character of their instrument are less than the current statistical errors. The collection rate for events with E > 10^{10}GeV has been ∿ 1 per month during the first 1.5 years of operation. This is about the same rate that has been maintained at Haverah since 1963 and at Yakutsk since 1974. The on-time appears to be averaging 7 percent.

5.5 Alternatives to harmonic analysis: results for the highest energies. The limitations of harmonic analysis when applied to directional data from modern air shower arrays have been appreciated by all those who have used them, but no obviously best alternative has yet emerged. Krasilnikov, for example, favors comparisons between opposite hemispheres or other broadly defined regions, selected according to astrophysical criteria. He points out as others have done that an energy-dependent anisotropy implies the possibility of differences in the energy spectra of cosmic rays from different parts of the sky. Some of his comparisons suggest that there may be real differences of this kind, but as yet the statistical errors are too great to allow drawing firm conclusions (Krasilnikov et al. paper OG4-29).

The main problem in making more fine-grained comparisons of this kind is predicting exactly how a given array will respond to isotropic primaries; i. e, predicting the denominator in the ratio (number observed/number expected). The Leeds group has worked out a refined method of doing this empirically (Astley et al. 1981). Similar results have been obtained by the Sydney and Yakutsk groups using Monte Carlo simulations (conference papers OG4-30 and 32). Most of the studies concern galactic latitude; no correlations with galactic longitude have been found by this method. The Leeds group has reported finding that the above ratio has a gradient: in general more showers arrive from southern than from northern galactic latitudes. But this gradient is energy dependent: as the energy increases the magnitude of the gradient first increases while the sense remains the same, and then there is a reversal so that above 10^{10}GeV more showers arrive from northern than from southern latitudes. Hillas (1982) has shown that the southern excess can be explained in terms of a radial cosmic ray density gradient within the galactic disc.

A southern excess below 10^{10}GeV had been reported once previously (Delvaille et al. 1962), but aside from that one instance there had been no confirmation prior to this conference. Now in paper OG4-30 Efimov et al. also report a southern excess. But they do not find a reversal; the Haverah northern excess appears at energies beyond the range of the Yakutsk data. The 140 large events reported by the Sydney group show no galactic gradient.

Efimov et al. make several other comparisons. They find that the Yakutsk data support those from Haverah and Volcano Ranch in showing an excess intensity of very large showers ($E > 2\text{-}3\cdot10^{10}$GeV) from directions within 45° of Virgo. However the Yakutsk data (22 events with $E > 2\cdot10^{10}$GeV) show a mild enhancement of intensity within ± 30° of the galactic equator whereas the combined Haverah-Volcano Ranch data show a pronounced depletion. In the latter case the observed ratio is 0.6 vs 1.6 expected, for 43 events with $E > 4\cdot10^{10}$GeV, chance probability 0.004 (Cunningham et al. conference paper OG4-33).

The northern excess, the deficit near the galactic equator and the presence of a large first harmonic amplitude are different ways of describing the same feature, one which I referred to previously as a large, rather diffuse cluster of directions centered between the galactic north pole and the galactic anticenter. Similarly the prominent sidereal second harmonic in the SUGAR data is an expression of two clusters about 12 hours apart, one near the spiral-out direction 7.8 hr, -26° (or the Vela SN remnant, 8.5 hr, -45°), the other in a direction that has no other known astrophysical significance. It is a striking feature of the SUGAR data that 5 of the 10 most energetic events, calorimetric energies all $> 10^{11}$GeV, have directions within $\sim$ 20° of the center of one of these clusters (A), while 2 of the remaining 5 are equally near the center of the other (B) (Horton et al. paper OG4-32). It was shown previously that the enhancement near 9 hr, -35° (cluster A) extends over a wide range of energies, perhaps down to 10^{7}GeV (Bray et al. 1981). The 10 highest-energy events in the northern hemisphere also seem to form two clusters; one associated with the northern excess, the other centered near 22-23 hr, 30° (Cunningham et al. paper OG4-33).

6. NEUTRAL PRIMARIES

6.1 Gamma-rays. The exciting news about γ-rays from Cygnus X-3 with an extraordinarily hard energy spectrum extending up to $\sim 10^{7}$GeV will be dealt with by another rapporteur (see numerous papers in Session XG4, especially XG4-14 and 15 by Samorski and Stamm and XG4-24 by Lloyd-Evans et al.)

Obviously a very effective way to improve the signal-to-noise ratio, in looking for similar but weaker sources, is to discriminate against nucleus initiated showers on the basis of structural features. In this connection an interesting result given at this conference in the air shower sessions is one by Stamenov et al. setting a limit of 0.1% on the intensity of > 10^6GeV γ-rays, averaged over all times and all directions in the northern hemisphere, compared to nuclei (paper EA1.1-32). In a recent paper Wdowczyk and Wolfendale (1983) suggest that the actual intensity of such γ-rays is not far from this limit, and they call attention to a number of consequences.

It is less obvious but also important that for the first time one can isolate a sample of air showers (for example those from the direction of Cygnus X-3 during certain time intervals) some of which, a determinate fraction, are produced by primaries of a distinctive type (γ-rays) rather than by some mixture of nuclei. A study of structural details in such a sample, with its built-in 'control group', can be especially fruitful for testing particle physics models. It should be possible to test experimentally predictions of the line width ($\sigma_\gamma|_{xmax}$, $\sigma_\gamma|_{N\mu}$) for pure γ-showers, something that cannot be done for any specific *nucleus* with present methods.

The Lodz group has analyzed more data and continues to find an excess intensity from the direction of the Crab Pulsar (or Nebula) for E $\sim 10^7$GeV. The showers giving the excess are somewhat μ-deficient (Dzikowski et al. conference paper OG4-22). The amplitude of the excess is great enough so that it would have been marginally detectable in the Cornell experiment (Delvaille 1962, see Fig. 19). In fact the phase angle of the first harmonic at that energy is not far from the right ascension of the Crab (8.1 ± 2.7 hr as against 5.5 hr). Data from the 150 m array at Haverah show no effect but the statistics are still sparse in the declination band where the effect is expected ($\sim$22°). The Akeno search for anisotropy of μ-poor showers does not extend to energies this low (paper OG4-23). Fly's Eye results on 10^6GeV γ-rays from the same part of the sky are given in conference paper XG4-19. These results, as well as others at lower energies, indicate that the source of γ-rays is variable.

Conference paper OG4-27 by Gerhardy and Clay reports a search for small scale anisotropies in the southern sky, with an interesting result that an almost significant excess intensity was observed in the direction of Centaurus A. Gamma-rays from this source have been observed at $\sim 10^3$GeV but they are not expected at the energy used for this search (10^7GeV) because of attenuation by collisions with 3° blackbody photons. In a related paper these authors point out that an excess intensity has been seen in the same general direction by two earlier experiments (Clay et al. 1983).

In paper OG4-24 Morello et al. give preliminary results of a search for anisotropies in smaller air showers (E $\sim 3\cdot10^4$GeV) at Plateau Rosa (3500 m a.s.l.) Fast timing is used to obtain angular resolution of order 5-10°, a considerable improvement over other experiments at this energy. Reasonable values have been obtained for the first and second sidereal harmonics as a function of declination. The array is intended primarily for studying γ-ray sources. In paper OG4-25 these authors describe a similar array they have put into operation at Chacaltaya, 5200 m a.s.l. At this elevation they estimate the energy threshold to be $\sim 10^3$GeV. With this instrument they hope to detect a high energy counterpart of γ-ray bursts seen by satellites.

6.2 Neutrinos. Turning to another type of neutral particle, there are new reasons for being optimistic that air showers produced by cosmic neutrinos will be discovered within the next decade. The neutrinos in question are decay products of pions produced in collisions between cosmic ray protons and photons of the 3° blackbody radiation. For kinematic reasons these neutrinos are quasi-monoenergetic with a median energy of about 10^{10}GeV. The intensity of these neutrinos according to a calculation by Stecker (1979) is shown in Figure 20.

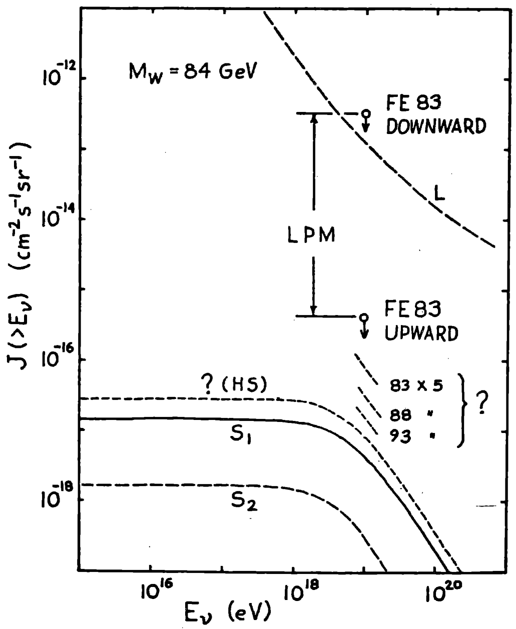

Fig. 20. Energy spectrum of cosmic neutrinos from collisions with 3° blackbody photons, and experimental flux limits. Curves S_1 and S_2 are by Stecker (1979) for two assumed cosmic ray spectra. S_1 corresponds to the spectrum incident on earth according to the best current evidence. HS is 2 times higher to allow for an evolutionary effect pointed out by Hill and Schramm (FERMILAB-Pub-83/49-THY, 1983; see also paper OG8-2). The experimental limits FE 83 DOWNWARD, UPWARD are the results of Cady et al. (paper MN4-15). Other markings are explained in the text.

Important advances have been made recently in reducing the uncertainty of this prediction: 1) there is better evidence that most of the highest energy particles are indeed protons, as required, 2) it follows from this and the evidence of anisotropy that these primaries are extragalactic, as required, 3) the anisotropy pattern suggests that the highest-energy particles reaching earth are produced far away in active galaxies; thus the average proton flux is likely to be greater, not less, than the local flux, 4) a sizeable discrepancy in measurements of the local flux has been resolved; the higher of the two alternative spectra assumed by Stecker is found to be correct, 5) a re-examination of the method used by Stecker suggests that the production of neutrinos may have been under-estimated by a factor of 2 or more (Hill and Schramm 1983). And of course the theoretical basis for predictions of ν interaction cross sections has been strengthened greatly by the discovery of the W_o and Z_o bosons.

The predicted cross sections are so small, $\sim 10^{-33}cm^2$ at $E_\nu = 10^{10}$GeV, that the target mass must be made very great. Showers of the indicated energy can be detected at long range by means of air fluorescence, but the total mass of air that can be monitored in this way is too small by several orders of magnitude. A very large increase can be achieved by exploiting the LPM (Landau-Pomeranchuk-Migdal) effect. This effect allows electrons produced by upward-moving neutrinos to emerge from the earth's crust with most of their energy intact, for ν_e-rock collisions within several hundred meters of the surface. Its significance in the context of DUMAND was pointed out by Markov and Zheleznykh (1979) and Dedenko et al. (1981). Application to the University of Utah Fly's Eye was proposed by Sokolsky (1983).

Experimental limits on neutrino intensity reported by the Utah group at this conference are also shown in Fig. 20 (Cady et al. in paper MN4-15). The point marked 'downward' is for observations of nearly horizontal showers initiated in the atmosphere; the one marked 'upward' is for upward showers initiated in the crust with development retarded by the LPM effect. The $3.9 \cdot 10^6$s running time was accumulated during the first 2 years of operation with an efficiency that can be expected to improve. The ν-N cross section is assumed to be $10^{-33}cm^2$. The dashed curve marked L is one that I calculated some time ago showing the limiting intensity for no observed downward events in 1 year, taking into account the energy dependence of the ν-N cross section and of the Fly's Eye response function but evidently over-estimating the acceptance solid angle. It is shown to emphasize that this opportunity of detecting cosmic neutrinos is rather sharply limited to energies above $\sim 3 \cdot 10^9$GeV.

The authors of the Fly's Eye report express confidence that through further efforts in matching the response of their detector to LPM-modulated cascades they will increase the sensitivity to upward events by a factor of $\sim$ 5. The effect this would have in relation to the predicted intensity is shown by the line-segment marked '83 x 5'. The effect of continuing to run the experiment without any further improvements until 1988 and 1993 is also shown.

If it is found that these neutrinos are not present, even with the minimum predicted intensity, then one will be required to renounce well-established views about the way 3° photons and highest-energy cosmic rays are distributed in the universe. If these neutrinos are found at all, whatever their intensity, their directional distribution will be a topic of the greatest astrophysical interest. The Fly's Eye is capable of determining air shower directions within a few degrees. Although the air fluorescence technique is well suited to this kind of search, and the Fly's Eye has the clear advantage of already being in operation, there are alternative methods which might eventually be used for the same purpose (Linsley 1983).

7. NEW PROJECTS

Much of the material that belongs under this heading is treated in a review I have already contributed to the proceedings of a 'mini-workshop', held in Bangalore during the cosmic ray conference, on "A New Generation of Antiproton-Proton Colliders and Cosmic Ray Interactions in the 5×10^{16}-10^{18}eV Region", to be edited by D. Cline and published by the University of Wisconsin. One new project discussed there, the ANI experiment, will give improved information on the high energy hadron component of air showers up to primary energies somewhat past the knee (Danilova et al. conference papers HE8-1 and 3). A new technique which may eventually allow such studies to be extended to even higher energies is one based on thermoluminescent sheets. Progress in perfecting and applying this technique is reported in a number of conference papers (see for example Okamoto et al. paper T6-4).

Although the trend is toward higher energies, the Adelaide group describes additions being made to its Buckland Park array for extending the response in the other direction, to lower primary energies (Prescott et al. paper EA5-1). An interesting new method of measuring air shower directions, intended for application to small size showers, is described by Liu et al. (paper T5-2).

The possibility of detecting very large air showers ($E > 10^{11}$GeV) by acoustic or radio methods continues to be explored but there are no positive results as yet (Kaneko et al. paper EA5-4).

A group at Gulmarg in Kashmir believes it has detected atmospheric fluorescence from large air showers using a very simple system like the one tested unsuccessfully in Ithaca prior to construction of the Cornell University Fly's Eye detectors (Bhat et al. paper EA4-23). As in case of the earlier work, filters are used to help separate the distinctively short-wavelength fluorescent light from Cerenkov light and other forms of background (Bhat et al. paper T1-15). The Utah group intends to instal similar filters, and hopes thereby to improve the performance of its fluorescence detectors.

Meanwhile two groups are preparing to enlarge their arrays of particle detectors. The Akeno group will first add four 2.25 m^2 scintillators outside the existing densely instrumented 1 km^2 array. Then, guided by information furnished by these units it plans to add $\sim$ 15 more of them, using optical fiber cables for data transmission, so as to achieve a sensitive area of $\sim$ 20 km^2 within a few years (Hara et al. paper EA1.2-2). The Leeds group describes a plan to enlarge the Haverah array to $\sim$ 100 km^2 by re-deploying about half of the existing water-Cerenkov tanks (total area 500 m^2) and supplying them with 'stand-alone' electronics, in a system resembling somewhat the one used in the SUGAR experiment (Brooke et al. paper T5-1).

By the time of the conference the Leeds group had modified its plan so as to make use of a suggestion for exploiting pulse width information as well as pulse height information in estimating the size of large showers (Linsley 1983). When making this suggestion I had in mind primarily the application to small arrays like those already in use, or being planned, for the purpose of studying γ-ray sources and general anisotropy in the 10^3-10^6GeV region. Among the millions of signals produced by each array of this kind there will be buried a few that are produced by very large showers, say $E > 10^{10}$GeV. In at least some instances it will be feasible to add, at very small cost, equipment for automatically singling out events in which the pulse widths are unusually great, say 100's of nanoseconds rather than just a few. Small showers cannot produce such signals; they must be due to large showers with large ($\sim$ 1 km) impact parameters. It may be feasible to record, in these rare cases, enough supplementary information (total pulse height plus some measure of the local particle direction) so that the primary energy and direction can be found. According to my estimates this can be done accurately enough to be useful for studying the very high energy anisotropy. I estimate that the counting rate of a very small array ('mini-array') using this principle will be 2-3 per year for $E > 10^{10}$GeV and 1 in several years for $E > 10^{11}$GeV. These rates are very small, but there already exist a dozen or more small arrays that are candidates for this application, with more on the way. My hope is that groups with small arrays will join together in a world-wide collaboration, perhaps using as a model the world-wide network of cosmic ray neutron monitors.

The method requires calibration, and as always the resolving power is limited by fluctuations in shower development. The information I had to start with came from photographic records of the Volcano Ranch experiment. The time resolution is poor and the dynamic range is very limited. By the time of the conference a substantial amount of additional data had been obtained by the Leeds group (Astley et al. paper EA1.2-5) as well as some by the Akeno group (Enoki et al. paper EA1.2-18, Hara et al. paper EA1.2-2). Preliminary results of applying the suggestion to a typical small array were reported by Hazen and Hazen (paper EA1.1-12). Since the conference additional data have been submitted for publication by Clay and Dawson of the Adelaide group.

Application of the new principle to the existing array at Haverah is straightforward. The array consists of a heavily instrumented central region plus six outer clusters of large detectors; that is, seven potential mini-arrays. The Leeds group has verified by means of experimental cross-checks that timing information from a typical cluster gives the shower direction accurately enough for anisotropy work, at ranges (impact parameters) up to $\sim$ 2 km (Watson, private communication). Thus by merely supplying the outer clusters with suitable transient recorders the effective area of the existing array will be more than tripled for energies above 10^{10}GeV. Such an array of mini-arrays is a form of 'stepped density' array (Linsley 1983) with the useful property of being sensitive over a very wide primary energy range.

8. HISTORICAL NOTES

As a rule dedications are not made in publishing scientific work, but in case of this section I will risk taking such an unusual step. These few notes are dedicated to Bruno Rossi and Pierre Auger, two pioneers in the study of air showers, not because of their scientific contributions, great as they are, but because one of them has been a dear friend for many years, while the other gave me new heart to go on when my need was greatest.

8.1 Energy calibration. It is interesting to see what sort of change there has been in estimates of the energy needed to produce typical air showers. A sensitive test (because $|\Delta J/J| > |\Delta E/E|$) is to compare intensities corresponding to a given threshold energy. This is done in Figure 21 for an energy, 10^6GeV, where in fact the calibration problem is relatively difficult because even at mountain elevation the showers are past maximum development. The estimate by Auger and his colleagues is remarkably close under the circumstances. It is taken from a report given in 1939, only a year later than their discovery of these showers. The first three estimates were made assuming

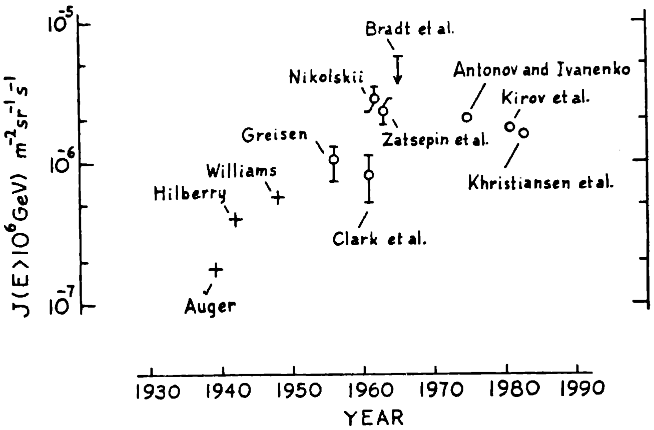

Fig. 21. Landmarks in determining the all-particle cosmic ray spectrum. J is the integral intensity at 10^6GeV, somewhat below the knee energy. The estimates made prior to 1950, shown by crosses, assumed electron primaries. With one exception (Clark et al.) the remaining values are for calorimetric measurements requiring no particle physics model or primary composition model.

electron primaries. The next point, due to Greisen, is the first one to take into account the division of energy among divers components, using measurements at mountain elevation as well as at sea level. The point due to Clark et al. is from the first experiment in which the size and direction of showers were measured on an individual basis. The points of Nikolskii and Zatsepin et al. are calorimetric, like Greisen's. They mark the first use of atmospheric Cerenkov radiation to estimate E_{EM}, the dominant term in the expression for the total deposited energy. The upper limit by Bradt et al. is from the first ground-based experiment in which (at somewhat higher energies) the electron maximum could be seen, so that E_{EM} could be derived from N_{max}. The manner in which later experiments (the last 3 points) appear to converge toward an intermediate value indicates to me that the chance of any substantial revision in the future is quite small.

8.2 Discovery of the knee. The earliest discussion I have found in which spectral kinks (both N_e and N_μ spectra) are attributed very probably to a steepening of the primary energy spectrum is by Miura and Hasegawa (1962). The kink in the electron size spectrum has a much longer history. At the 1959 conference in Moscow the MSU group reported a steepening of the sea level size spectrum for $N_e > 8 \cdot 10^5$ but no steepening was found at Pamir (3860 m a.s.l.) in the range $2.5 \cdot 10^4 < N_e < 1.3 \cdot 10^7$ (Kulikov et al. 1960). A group working at Norikura (2770 m a.s.l.) reported a steepening from integral exponent 1.55 to 2.04 occurring for N_e between 3 and $5 \cdot 10^5$ (Kameda et al. 1960). Neither group drew any conclusions. I noticed only recently that this kink was undoubted-

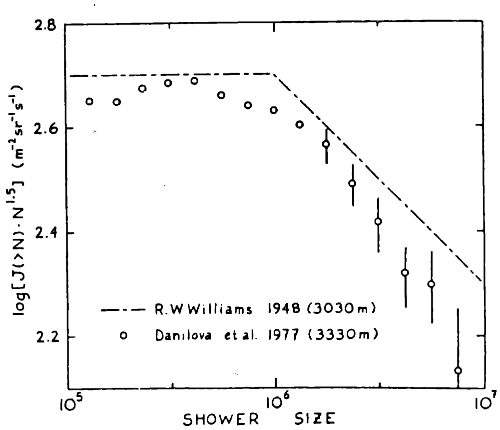

Fig. 22. The discovery of the size spectrum kink. The circles are a modern result at practically the same elevation.

ly seen much earlier by R. W. Williams in the experiment which first located individual shower cores from symmetry (Williams 1948). His result, derived from a density spectrum, is shown without any renormalization in Figure 22, together with a recent result at almost the same elevation.

8.3 Calorimetric energy scale. This began as the problem of energy balance. Rossi had noted in 1948 that the flux of energy incident on the earth, as calculated from the primary energy spectrum, was greater than could be accounted for at that time in terms of spectra of secondary components measured at various levels in the atmosphere. Following the discovery of neutral pions in 1950 it was possible to make better sense out of the low energy atmospheric cascade (Komuri 1955, Puppi 1956). By 1957 the inital discrepancy had been explained satisfactorily (Webber 1957). Meanwhile, the point had been made by Cocconi (1950) that any particle observed in the lower atmosphere is in a sense part of an extensive air shower. The fact that the energy balance is satisfactory at low energies, where the atmospheric cascade is relatively complex, would naturally suggest using it at much higher energies to determine the incident flux. (The strong forward collimation of secondary particles at very high energies is helpful; so is the relative unimportance of the N-component.) Figure 23 is a copy of Fig. 7 with the energy scale extended down to low energies, showing the result obtained by Puppi for E_{EM}/E, the fraction of incident energy deposited by electrons. The curve is for a cascade simulation by Hillas (1981), who happened in this case to publish values of this interesting quantity, which he had calculated for an unusually wide energy range. The disagreement between the curve and the experimental points at very high energies is expected for the model he used, scaling with constant cross sections. The agreement at the low-energy end, where the model is valid but the calculations are more difficult, is impressive.

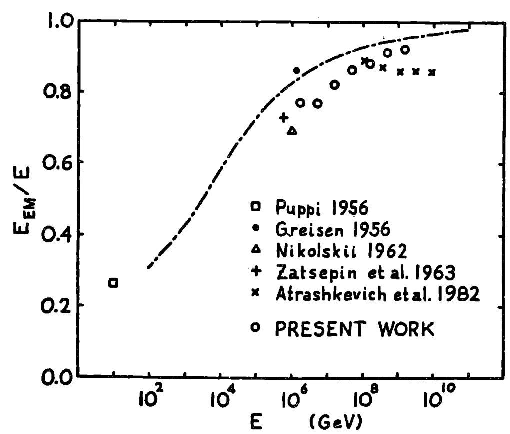

Fig. 23. Fraction of primary energy given to the soft component, with a low-energy result by Puppi.

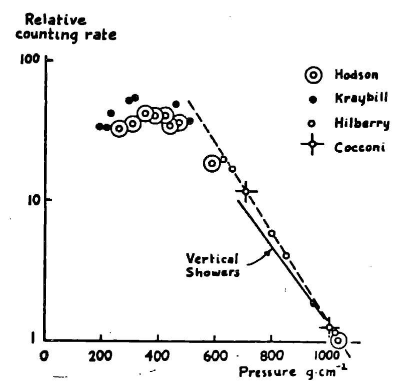

Fig. 24. Early results on longitudinal development, from Wilson (1956).

8.4 Longitudinal development. The fact that even before 1950 some difficult measurements were made rather well is shown in Figure 24. It is taken from a 1956 review by J. G. Wilson but the data are earlier. There is a remarkable superficial resemblance to much later results shown in Fig. 3

of conference paper EA1.1-14 (integral intensity for $N > 10^6$ vs observation depth, summarized by Antonov et al.) Clearly these early data have something to do with the shower profile, a curve which shows the way showers grow to a maximum size and then diminish. But to go from the one to the other requires so much additional detailed knowledge, about the all-particle spectrum, about the lateral structure of showers and its altitude dependence, and about the response of specific counter set-ups, that we believe in the possibility now only because the answer has already been found in other ways.

The idea of using N_{max} as a measure of E_{EM} and hence of E seems to have been discussed first by Clark (1962). He suggested the value 2 GeV/particle for the N_{max} to E conversion factor, a value I was guilty of supporting up to the time of this writing as reasonable in case of the largest showers at least. I showed in Part 2 that this factor depends on the value of $E_{\mu\nu h}$, which one has tended to over-estimate. But for very large showers it depends mainly on E_{EM}, which one will get about right if one knows N_{max} and x_{max}. Realizing this, Clark bravely did his best to estimate what would nowadays be called the elongation vs energy relation, with very approximate information to go on. I show his result here because it is the first of its kind that I know of, and because through no fault of Clark's it would be hard for others to recognize it. The variables he used are x_{max}, "the atmospheric depth at which $(\partial N/\partial x)_s = 0$" (where s is shower size) and N_{max} (rather than E, but we recall that the conversion factor is given elsewhere in his paper). However x_{max} is the ordinate, not the abscissa. Moreover, in publication the caption belonging to this figure was interchanged with another. Clark's estimates as they would be shown today are given in Figure 25 together with some recent data. The lowest-energy point is taken from observations of the zenith angle distribution of small showers carried out with a spark chamber in an airliner by Kamata et al. The next point, which agrees quite well with recent ones, is taken from the zenith angle distribution of much larger showers at El Alto in Bolivia (630 g/cm^2). The third point, which does not agree as well, is from my own similar observations at Volcano Ranch. The fourth is derived, by extrapolation, from measurements of zenith angle distributions and barometric coefficients at Cornell. How helpful it would have been, in that era, to have known about theoretical constraints on the elongation rate!

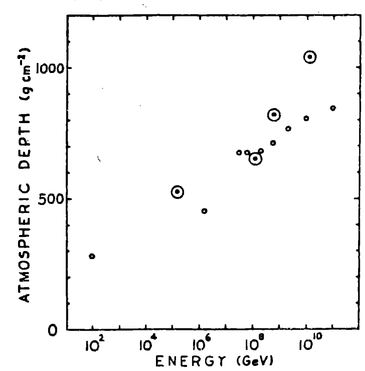

Fig. 25. Early results on the level of maximum shower development (large circles), from Clark (1962). The small circles are modern results quoted by Linsley and Watson (1981).

8.5 *Osservazione*, Asmara (Somalia). "The frequency of coincidences registered with the counters far apart from each other, shown in the tables as 'accidental coincidences', seems to be higher than would have been predicted from the resolving time of the electronic circuits, measured at Padua before leaving ($2 \cdot 10^{-4}$sec for circuit II). This makes one suspect that such coincidences were not, in reality, wholly accidental. This hypothesis seems to be strengthened by the two following observations:"

" 1st) In 21 hours and 37 minutes there occurred 14 coincidences among 3 counters that were separated and arranged so that a single particle was not able to go through all of them. If these were to be considered as accidental, one would have to attribute to the circuits a resolving time of about 0.02 s. But in this case there would have to occur, between two shielded counters, about 200 chance coincidences per hour, while in reality only 6 are observed.

2nd) When in one of the two circuits the counters were set up to register double 'accidental' coincidences, the infrequent coincidences signalled by this circuit were often accompanied by a simultaneous coincidence in the other circuit."

"It would seem, therefore (since suspicion about possible outside disturbances had been ruled out by appropriate control experiments), that from time to time there arrive upon the equipment very extensive groups of particles [*sciami molto estesi di corpuscoli*] which produce coincidences between counters even rather distant from each other."

"I did not have enough time to study this phenomenon further in this place so as to establish with certainty the existence of the supposed groups of particles and to investigate their origin." (Rossi 1934)

(See also p. 181 in Rossi's paperback, Cosmic Rays, published in 1964. In translating the word *sciami* I have used 'groups', following Rossi. My Italian-English dictionary suggests 'swarms'.

CONCLUSIONS

The problem of measuring the all-particle energy spectrum appears to be solved, as well as this can be done with present day methods, up to the region of the ankle, where better statistics are needed and a discrepancy between Yakutsk results and others needs to be explained.

In the region of the knee it should be possible with ground-based experiments to make a definite choice between alternatives as broadly different as $\langle a \rangle > \sim 2$. ('Fe enhancement), $\langle a \rangle \sim 1.5$ ('no change') and $\langle a \rangle < \sim 1$. ('proton enhancement'). However the situation in this region is probably so complex that the effort needed in order to track the elemental spectra through it by means of a large-scale, long-duration experiment in space is indispensable (see Müller 1982, Ormes 1982 for descriptions of equipment now waiting to be launched). Meanwhile, the information being provided by balloon-borne emulsion calorimeters is extremely valuable.

At higher energies the primary mass resolution of ground-based experiments tends to improve. In time it may be possible to measure $\langle a \rangle$ in this region to an accuracy of ± 0.2. Those interested in using the cosmic ray beam to study nucleus-nucleus collisions are probably safe in assuming that useful numbers of heavy nuclei are present up to 10^7GeV/particle and that it will be possible with sufficient effort to distinguish between the showers they produce and those produced by protons. The problem of determining the proton-alpha ratio above the knee is a formidable challenge.

The study of cosmic ray anisotropy in all its aspects seems to offer especially great opportunities. It is already seen from the γ-ray discoveries that early hints of narrow-angle anisotropies had some basis in reality. These results failed to be more convincing because the experiments were done in isolation from one another, so that time-variability, to the extent it is present, was an insurmountable difficulty. Enough groups are now involved so that their observations will begin to overlap in time as well as in direction and energy, as required if one is to separate real sources from spurious ones. However, beginning about 10^5GeV the experiments must either be individually large-scale or else quite numerous. If one uses as a test the ability to detect the sidereal time variation by means of harmonic analysis, then the total sensitive area needed to achieve a signal-to-noise ratio of 3 in 1 year increases from about 50,000 m^2 at 10^5GeV to 5 km^2 at 10^8GeV. One must strive, in these experiments, for an angular resolution of a few degrees or better, and for an energy resolution of 50% or better.

For the highest energies ($E > 10^{10}$GeV) the total sensitive area in use world-wide will soon be increased to exceed 100 km^2. Within the next decade this figure may grow to 1000 km^2.

ACKNOWLEDGEMENTS

I am grateful to the National Organizing Committee for inviting me to be a rapporteur. I thank A. Buffington and others of the APS Division of Cosmic Physics for travel support. Support for this work was also provided by the National Science Foundation (Grant No. PHY-8213331).

APPENDIX: AIR SHOWER MEASURES OF PRIMARY COMPOSITION

Let y be an air shower observable whose distribution for proton-initiated showers of a given energy is $f_1(y)$. I will say that this distribution represents a *line* (proton line) whose intensity, location and width are given by

$$w_i = \int f_1(y)dy \ , \qquad \text{(A1)}$$

$$\langle y \rangle_1 = \int y f_1(y)dy / \int f_1(y)dy \ , \qquad \text{(A2)}$$

and

$$\sigma_1 = [\int (y-\langle y \rangle)^2 f_1(y)dy / \int f_1(y)dy]^{\frac{1}{2}} \ , \qquad \text{(A3)}$$

respectively. The corresponding distribution for showers produced by primary nuclei with a mixed composition will be a superposition of such lines.

If the lines had negligible width, then, letting w_i, y_i represent the intensity and location of the i-th line, and the total intensity be normalized to unity, one would have, again by definition,

$$\langle y \rangle = \Sigma w_i y_i \ , \qquad \text{(A4)}$$

and

$$\sigma_y^2 = \Sigma (y_i - \langle y \rangle)^2 w_i = \Sigma y_i^2 w_i - \langle y \rangle^2 \ . \qquad \text{(A5)}$$

For lines of finite width the centroid (center of gravity) of the entire spectrum is given by

$$\langle y\rangle = \int y\Sigma f_i dy/\int\Sigma f_i dy = \Sigma w_i \langle y\rangle_i \ . \qquad \text{(A6)}$$

The variance (width squared) of the entire spectrum is

$$\sigma_y^2 = \int (y-\langle y\rangle)^2 \Sigma f_i dy/\int\Sigma f_i dy \ . \qquad \text{(A7)}$$

By writing out the square, substituting from the previous equations, and rearranging terms one obtains

$$\sigma_y^2 = \Sigma w_i \sigma_i^2 + \Sigma w_i \langle y\rangle_i^2 - \langle y\rangle^2 \ . \qquad \text{(A8)}$$

The first term on the right is the average width of the lines. Referring to (A5) one sees that the remaining terms represent the variance of the line locations, which I will denote by σ_ℓ^2. This tells us that the variance of the entire spectrum consists of two parts, one due entirely to fluctuations, the other due entirely to the width of the primary mass spectrum. Sometimes one may predominate and sometimes the other, depending on the choice of shower observable. Note that the only requirement on the distributions f_i is that they be reasonably well behaved; they need not by any means be Gaussian.

I will assume that over a sufficiently wide energy interval (2 decades or more) the mean value of y for proton initiated showers can be graphed vs logE as a straight line:

$$y_1 = y_o + b\cdot \ln E \qquad \text{(A9)}$$

where y_o and b are constants, independent of energy. Practically all observables that are used to study primary composition by means of air showers have this character; examples are the elongation x_{max} and $\log N_\mu$ where N_μ is the muon size. Note, comparing (A9) with (A2), the change of notation: from here on, y_i denotes the average for the i-th component (average over f_i, the line shape). The symbol < > will refer henceforth to an average over the index i; that is, an average over the primary mass spectrum.

Next I will make use of the superposition principle, according to which *an average shower produced by a nucleus with energy E and mass number A is indistinguishable, except in early stages of development, from a superposition of A average proton initiated showers, each with energy E/A*. In applying this principle I must follow Peters in observing a distinction between observables of two types (Peters 1960). Those he called type G depend only on the primary energy per nucleon; for a given E/A they are independent of A; an example is the shower elongation x_{max}. Those he called type F are proportional to A; examples are N_e and N_μ. The ratio of two type-F observables belongs to type G.

Many type-G observables also have the property described by (A9): they are approximately linear functions of lnE. It follows from superposition that in such cases the separation between various lines depends on particle physics only through the rate parameter b. It depends logarithmically on the primary mass difference:

$$y_i - y_j = -b\cdot(a_i - a_j) \ , \qquad \text{(A10)}$$

where $a = \ln A$. If Y is a type-F observable the present analysis can still be applied to its logarithm, provided that lnY for proton showers is an approximately linear function of lnE. In this case I will call lnY a 'type-H' observable. Superposition gives

$$y_i - y_j = (1-b)(a_i - a_j) \ . \qquad \text{(A11)}$$

Substituting into (A6) the appropriate expression for y, one finds the following 'master equation' for the centroid of the observed y distribution:

$$\text{for type G,} \qquad \langle y \rangle = y_o + b(\ln E - \langle a \rangle) \ ,$$

$$\text{for type H,} \qquad \langle y \rangle = y_o + b \cdot \ln E - (b-1)\langle a \rangle \ . \qquad \text{(A12)}$$

Using (A12) one can express σ_ℓ above in terms of the rate parameter and σ_a, the dispersion of lnA relative to <lnA>, which I will call the 'logarithmic dispersion' of the equal-energy mass spectrum.

$$\text{For type G,} \qquad \sigma_\ell = b \cdot \sigma_a \ ,$$

$$\text{For type H,} \qquad \sigma_\ell = |b-1|\sigma_a \ . \qquad \text{(A13)}$$

The line widths σ_i arise from fluctuations, primarily in the starting depth but also in the subsequent development of showers. The dependence on A of the average starting depth is given approximately by the cross section formula of Bradt and Peters (1950):

$$\text{cross section} = \pi r_o^2 (A_1^{1/3} + A_2^{1/3} - \beta)^2 \ , \qquad \text{(A14)}$$

where the value of β, the overlap parameter, is ~ 1 (Lindstrom et al. 1975). According to this formula one might expect Fe lines to be only one fifth as wide as proton lines. Calculations in which the gradual nature of heavy nucleus fragmentation is taken into account predict a somewhat weaker A-dependence (Elbert et al. 1976, Ellsworth et al. 1982, Chantler et al. 1982). These results can be represented quite accurately by writing

$$\sigma_i = \sigma_1 (1 - k \cdot a_i) \ , \qquad \text{(A15)}$$

where the value of σ_1 depends on the choice of observable and the value of k lies in the range $0.15 \pm .05$. Comparing calculations for different values of the p-air cross section one finds, as expected, that the value of σ_1 is nearly proportional to the p-air interaction mean free path (Walker and Watson 1982, Linsley 1982). The parameter k is also model dependent but only weakly so. Using (A15) one finds that the average line width is given by

$$\Sigma w_i \sigma_i^2 = \sigma_1^2 (1 - k\langle a \rangle)^2 + k^2 \sigma_1^2 \sigma_a^2 \ . \qquad \text{(A16)}$$

The first term on the right is just $(\sigma_{\langle a \rangle})^2$, the variance of a line having average a. Finally, substituting from (A16) and (A13) into (A8), one obtains the second master equation, which describes the variance of an observed distribution:

for type G, $\sigma_y^2 = (\sigma_{<a>})^2 + (k^2\sigma_1^2 + b^2)\sigma_a^2$,

for type H, $\sigma_y^2 = (\sigma_{<a>})^2 + [k^2\sigma_1^2 + (b-1)^2]\sigma_a^2$. (A17)

In general σ_y depends on both σ_a, the width of the primary mass distribution and, through fluctuations, on <a>, the average primary mass.

Strictly speaking these results apply only when events are selected on the basis of primary energy. Extension to other cases, for example to showers selected by size, is not difficult, but here I will only sketch what must be done. Assume that the selection is done on the basis of a second observable z which has the same character as y (cf. Eq. A9 and the accompanying text). The same considerations about mass dependence and fluctuations come into play; the only difference is that one has 2 dimensions (y,z) rather than one. The master equations corresponding to (A12) and (A17) will have the same form, with more or less altered coefficients for the composition-dependent quantities <a> and σ_a.

Development of this formalism began in the early 1960's for application to a measurement of the air shower 'muon content' (Linsley and Scarsi 1962), and has continued by fits and starts ever since (Linsley 1963, 1967, 1973, 1974, 1977a,b, Linsley and Watson 1981a, b, c, Linsley 1982).

REFERENCES: CONFERENCE PAPERS

Paper No.	Authors
OG4-2	Abulova, V.G. et al. (MSU emulsion calorimeter group)
OG4-8	Acharya, B., Rao, M.V.S., Sivaprasad, K. and Sreekantan, B.V.
HE5-17,18	Amenomori, M. et al. (Mt. Fuji collaboration)
EA1.1-14	Antonov, R.A., Fateeva, I.M. and Kuzmin, V.A.
EA1.2-5	Astley, S., Bower, A., Lambert, A., Linsley, J. and Watson, A.A.
EA1.1-34	Atrashkevich, V.B. et al. (MSU muon spectrometer group)
HE7.2-7	Battistoni, G. et al. (NUSEX collaboration)
EA4-23	Bhat, C.L., Sanecha, V., Mitra, A., Sapra, M. and Razdan, H.
T1-15	Bhat, C.L., Kaul, R.K., Sapra, M.L. and Razdan, H.
OG4-21	Bower, Cunningham, Linsley, Perrett, Reid and Watson
T5-1	Brooke, Linsley, Lloyd-Evans, Ogden, Patel, Reid and Watson
OG4-5	Burnett, T.H. et al. (JACEE collaboration)
OG4-18	Cady, B. et al. (Fly's Eye group)
OG4-31	Cady, Cassiday, Elbert, Gerhardy, Loh, Mizumoto, Sokolsky & Steck
MN4-15	Cady, Cassiday, Elbert, Gerhardy, Loh, Mizumoto, Sokolsky & Steck
XG4-19	Boone, Cady, Cassiday, Elbert, Loh, Sokolsky, Steck & Wasserbaech
OG6-1	Colgate, S.
OG6-4	Colgate, S.
OG4-33	Cunningham, G., Lloyd-Evans, J., Reid, R.J.O. and Watson, A.A.
HE8-1,3	Danilova et al. (ANI collaboration)
EA1.2-12	Diminstein, O.S. et al. (Yakutsk group)
EA1.2-10	Dyakonov, M.N. et al. (Yakutsk group)
OG4-22	Dzikowski, Gawin, Grochalska, Korejwo and Wdowczyk

REFERENCES - continued

Paper No.	Authors
EA3-15	Efimov, N.N. et al. (Yakutsk group)
OG4-15	Efimov, N.N. and Sokurov, V.F.
OG4-30	Efimov, N.N., Mikhailov, A.A. and Pravdin, M.I.
EA1.2-18	Enoki, Kakimoto, Inoue, Suga, Nishi and Nakatani
OG8-1	Fischhoff, E.
OG4-27	Gerhardy, P.R. and Clay, R.W.
EA4-4	Grigoriev, Efimov, Kalmykov, Nechin, Prosin and Fomin
EA1.2-2	Hara, Hatano, Hayashida, Honda, Ishikawa, Kifune, Nagano & Teshima
EA1.2-14	Hara, T. et al. (Akeno group)
EA3-14	Hara, T. et al. (Akeno group)
OG4-16	Hara, T. et al. (Akeno group)
OG4-23	Hara, Hayashida, Honda, Kamata, Kifune, Nagano, Tanahashi & Teshima
EA1.1-12	Hazen, W.E. and Hazen, E.S.
EA2-20	Hein, L.A. and Kanevsky, B.L.
OG4-20	Horton, L., McCusker, C.B.A., Peak, L.S., Ulrichs, J. and Winn, M.M.
OG4-32	Horton, L., McCusker, C.B.A., Peak, L.S., Ulrichs, J. and Winn, M.M.
EA1.2-15	Horton, L., McCusker, C.B.A., Peak, L.S., Ulrichs, J. and Winn, M.M.
EA5-4	Kaneko, T. et al. (BASJE collaboration)
HE4-33	Kempa, J. and Wdowczyk, J.
OG4-13	Khristiansen, G.B. et al. (MSU-Samarkand collaboration)
OG4-29	Krasilnikov, D.D. et al. (Yakutsk group)
T5-2	Liu Zhong-he, Bai Guangzhi, Li Guangju, Geng Qingxi and Liu Jianguo
XG4-24	Lloyd-Evans, J., Patel, M., Reid, R.J.O. and Watson, A.A.
OG4-1	MacKeown, Cawley, Clear, Fegan, Lamb, Turver and Weekes
EA3-1	McGaughan, J.B.T.
OG6-37	Meyer, J.P.
OG4-10	Mincer, Freudenreich, Goodman, Tonwar, Yodh, Ellsworth and Berley
OG4-24	Morello, C., Navarra, G. and Vallania, P.
OG4-25	Morello, C., Navarra, G., Miranda, P., Martinic, N. and Turtelli, A.
MG9-1	Nagashima, K., Ishida, Y., Mori, S. and Morishita, I.
MG9-2	Nagashima, K., Morashita, I. and Yasue, S.
OG4-12,14	Nikolskii, S.I. and Stamenov, J.N.
T6-4	Okamoto, Kawaguchi, Kino, Kitajima, Miono, Misaki, Muramoto & Saito
OG5.1-10	Ormes, J.F.
EA5-1	Prescott, Clay, Corani, Dawson, Gregory and Patterson
XG4-14,15	Samorski, M. and Stamm, W.
OG8-2	Schramm, D.N. and Hill, C.T.
OG6-22	Silberberg, R., Tsao, C.H., Letaw, J.R. and Shapiro, M.M.
OG4-9	Sood, R.K.
EA1.1-50	Sreekantan, B.V., Tonwar, S.C. and Viswanath, P.R.
EA1.1-32	Stamenov, J.N., Ushev, S.Z., Nikolskii, S.I. and Yakovlev, V.I.
OG4-11	Stamenov, Ushev, Janminchev, Nikolskaya and Pavliuchenko
OG5.1-9	Streitmatter, Balasubrahmanyan, Ormes and Protheroe
OG1-15	Streitmatter, Balasubrahmanyan, Mauger, Ormes and Stephens
EA1.2-11	Walker, R. and Watson, A.A.
EA3-23	Wdowczyk, J. and Wolfendale, A.W.

REFERENCES: PRE-CONFERENCE PAPERS

Acharya et al. (Kolar group) 1981, Proc. 17th ICRC (Paris) 9, 162.
Aguirre, C. 1982, Proc. Workshops on Cosmic Ray Interactions and High Energy Results, La Paz and Rio de Janeiro, ed. C.M.G. Lattes (Campinas) p. 404.
Alexeenko, Chudakov, Gulieva, Sborshikov 1981, Proc. 17th ICRC (Paris) 2, 146.
Allkofer et al. (Kiel group) 1981, Proc. 17th ICRC (Paris) 9, 174.
Anda et al. (BASJE group) 1981, Proc. 17th ICRC (Paris) 2, 164.
Antonov, R.A. and Ivanenko, I.P. 1975, Proc. 14th ICRC (Munich) 8, 2708.
Asakimori et al. (Kobe group) 1981, Proc. 17th ICRC (Paris) 11, 301.
Ashton et al. (Durham group) 1979, Proc. 16th ICRC (Kyoto) 13, 243.
Astley et al. (Leeds group) 1981, Proc. 17th ICRC (Paris) 2, 156.
Atrashkevich, Efimov, Khristiansen & Kulikov 1983, Invited Talks, 8th European Symposium, eds. N. Iucci et al. (Tecnoprint: Bologna) p. 67.
Auger, Ehrenfest, Maze, Daudin, Robley & Fréon 1939, Rev. Mod. Phys. 11, 288.
Bell, M.C., Kota, J. and Wolfendale, A.W. 1974, J. Phys. A 7, 420.
Berezinski, V.S. 1983 talk, 8th European Symposium, unpublished.
Bergeson, Cutler, Davis & Groom 1979, Proc. 16th ICRC (Kyoto) 4, 188.
Berkovitch, M. and Agrawal, S.P. 1981, Proc. 17th ICRC (Paris) 10, 246.
Blandford, R.D. and Payne, D.G. 1982, M.N.R.A.S. 199, 883.
Bower, Cunningham, Linsley, Reid & Watson 1983, J. Phys. G 9, L53.
Bradt, H.L. and Peters, B. 1950, Phys. Rev. 80, 943.
Bradt et al. 1965, Proc. 9th ICRC (London) 2, 715.
Bray et al. (Sydney group) 1981, Proc. 17th ICRC (Paris) 2, 168.
Burnett et al. (JACEE collaboration) 1983, Phys. Rev. Lett. 51, 1010.
Catalogue of Highest Energy Cosmic Rays No. 1, 1980, ed. M. Wada, World Data Center C2 for Cosmic Rays (Inst. of Physical and Chemical Research: Tokyo).
Cassiday et al. (Fly's Eye group) 1982, Proc. Workshop on Very High Energy Cosmic Ray Interactions, eds. M.L. Cherry et al. (Univ. of Penn.) p. 72.
Catz, Ph., Maze, R. and Gawin, J. 1970, Proc. 11th ICRC (Budapest) 8, 395.
Catz et al. (Verriéres-Lodz collab.) 1975, Proc. 14th ICRC (Munich) 12, 4329.
Chantler, Craig, McComb, Orford, Turver & Walley 1982, J. Phys. G 8, L51.
Cherry et al. (Homestake group) 1981, Phys. Rev. Lett. 47, 1507.
Cherry, M.L., Dar, A. and Bludman, S.A. 1983 preprint.
Cini-Castagnoli et al. 1975, Proc. 14th ICRC (Munich) 4, 1453.
Clark, G. 1962, J. Phys. Soc. Japan 17, suppl. A-III, 286.
Clay, R.W. and Dawson, B.R. 1983, submitted to Australian J. Phys.
Clay, Gerhardy and Liebing 1983, submitted to Australian J. Phys.
Cocconi, G. 1950, Phys. Rev. 79, 1006.
Colgate, S. 1975, Phys. Rev. Lett. 34, 1177.
Compton, A.H. and Getting, I.A. 1935, Phys. Rev. 47, 817.
Cunningham, Lloyd-Evans, Pollock, Reid & Watson 1980, Ap. J. 236, L71.
Danilova, Erlykin & Machavariani 1981, Proc. 17th ICRC (Paris) 6, 146.
Danilova et al. (USSR-Bulgarian collab.) 1977, Proc. 15th ICRC (Plovdiv) 8, 129.
Davies, Elliot & Thambyahpillai 1979, Proc. 16th ICRC (Kyoto) 4, 210.
De Beer, Holyoak, Oda, Wdowczyk and Wolfendale 1968, J. Phys. A 1, 72.
Daudin, J., Auger, Cachon and Daudin, A. 1956, Nuovo Cimento 3, 1017.
Davis, L. 1954, Phys. Rev. 96, 743.
Dedenko, Markov, Stern & Zheleznykh 1981, Proc. 17th ICRC (Paris) 10, 393.
Delvaille, Kendziorski and Greisen 1960, Proc. 6th ICRC (Moscow) III, 143.
Delvaille, J. 1962, Thesis, Cornell University.
Delvaille et al. 1962, Proc. 5th Inter-American Seminar on Cosmic Rays, La Paz, eds. I. Escobar et al. (Lab. Fisica Cosmica: La Paz) 2, XL-1.

REFERENCES: PRE-CONFERENCE PAPERS - continued

Dixon et al. (Durham group) 1974, J. Phys. A 7, 1010.
Dzikowski et al. (Lodz group) 1977, Proc. 15th ICRC (Plovdiv) 8, 46.
Efimov, N.N. and Pravdin, M.I. 1983, unpublished.
Elbert, J.W. 1982, Proc. Workshop on Very High Energy Cosmic Ray Interactions eds. M.L. Cherry et al. (University of Pennsylvania: Philadelphia) p. 312.
Elbert, Mason, Morrison & Narasimham 1976, J. Phys. G 2, 971.
Ellsworth, Gaisser, Stanev & Yodh 1982, Phys. Rev. D 26, 336.
Erlykin, A.D. and Kuzina, N.P. 1981, Proc. 17th ICRC (Paris) 5, 243.
Escobar, Nerurkar & Weil 1960, Planet. Space Science 2, 187.
Fenton, A.G. and Fenton, K.B. 1976, Proc. Intern. Cosmic Ray Symposium on High Energy Cosmic Ray Modulation, eds. K. Nagashima et al. (Tokyo) p. 313.
Fichtel, C.E. 1963, Phys. Rev. Lett. 11, 172.
Fujii, Z. 1971, Rep. Ionos. Space Res. Japan 25, 189.
Gaisser, T. 1979, Proc. Air Shower Workshop, University of Utah, ed. T.K. Gaisser (Bartol Research Foundation: Newark) p. 57.
——— 1981, Proc. 17th ICRC (Paris) 6, 233.
Gerdes, C., Fan, C.Y. & Weekes, T.C. 1973, Proc. 13th ICRC (Denver) 1, 219.
Giler, M., Wdowczyk, J. and Wolfendale, A.W. 1980, J. Phys. G 6, 1561.
Ginzburg, V.L. and Syrovatskii, S.I. 1961, Progr. Theor. Phys. Supp. 20, 1.
Gombosi et al. (Hungarian-Bulgarian collab.) 1975, Proc. 14th ICRC (Munich) 2, 586 and 1977, Proc. 15th ICRC (Plovdiv) 11, 109.
Greisen, K. 1956 in Progress in Cosmic Ray Physics, ed. J.G. Wilson (North-Holland: Amsterdam) p. 1.
——— 1960, Ann. Review of Nuclear Science 10, 63.
Grigorov et al. 1971a, Proc. 12th ICRC (Hobart) 5, 1746 and 1971b, ibid. 1752.
Hess, V.F. and Steinmaurer, R. 1933, Sitzungsber. Preuss. Ak. Phys.-Math. Kl. 15.
Hilberry, N. 1941, Phys. Rev. 60, 1.
Hill, C. and Schramm, D. 1983, FERMILAB-Pub-83/49-THY.
Hillas, A.M. 1978 in Cosmic Rays and Particle Physics-1978, ed. T.K. Gaisser (American Institute of Physics: New York 1979) p. 373.
——— 1981, Proc. 17th ICRC (Paris) 2, 125 and 13, 69.
——— 1981, Proc. Paris Workshop on Cascade Simulations, eds. J. Linsley and A.M. Hillas (TCAST: Albuquerque) p. 13.
——— 1982, in Composition and Origin of Cosmic Rays, ed. M.M. Shapiro (Reidel: Dordrecht)
——— 1983, Proc. Cosmic Ray Workshop, University of Utah, ed. T.K. Gaisser (Bartol Research Foundation: Newark) p. 1.
Hillas, Marsden, Hollows & Hunter 1971, Proc. 12th ICRC (Hobart) 3, 1001.
Hillas, A.M. and Ouldridge, M. 1975, Proc. 14th ICRC (Munich) 2, 623.
Jokipii, J.R. 1966, Ap. J. 146, 480.
Juliusson, E. 1975, Proc. 14th ICRC (Munich) 8, 2689.
Kakimoto et al. (BASJE collaboration) 1981, Proc. 17th ICRC (Paris) 11, 254.
Kameda, T., Maeda, T. & Toyoda, Y. 1960, Proc. 6th ICRC (Moscow) III, 58.
Karakula, S., Osborne, J.L. and Wdowczyk, J. 1974, J. Phys. A 7, 437.
Khrenov, B. and Linsley, L. 1981, Proc. 17th ICRC (Paris) 10, 354.
Khristiansen, G., Kulikov, G. & Fomin, J. 1980, Cosmic Rays of Superhigh Energies (Verlag Karl Thiemig: München) p. 132.
Király, Kóta, Osborne, Stapley & Wolfendale 1979, Proc. 16th ICRC (Kyoto) 4, 221.
Kirov, Stamenov, Ushev & Nikolskaya 1981, Proc. 17th ICRC (Paris) 2, 109.
Klemke et al. (Kiel group) 1981, Proc. 17th ICRC (Paris) 9, 150.

REFERENCES: PRE-CONFERENCE PAPERS - continued

Koch et al. (Saclay-Lyngby collaboration) 1981, Proc. 17th ICRC (Paris) 2, 18.
Komori, H. 1955, Progr. in Theor. Phys. 13, 205.
Krasilnikov, D.D. 1974 talk, 4th European Symposium on Cosmic Rays, Lodz.
Krys, Tomaszewski, Wrotniak & Wlodarczyk 1981, Proc. 17th ICRC (Paris) 5, 315.
Kulikov et al. 1960, Proc. 6th ICRC (Moscow) III, 85.
Lake, G. and Pudritz, R.E. 1983 preprint.
La Pointe et al. (BASJE collaboration) 1968, Can. J. Phys. 46, S68.
Lezniak, J.A. and Webber, W.R. 1978, Ap. J. 223, 676.
Lindstrom et al. 1975, Proc. 14th ICRC (Munich) 7, 2315.
Linsley, J. 1963, Proc. 8th ICRC (Jaipur) 4, 295.
——— 1967, Rev. Sci. Instrum. 38, 1268.
——— 1973, Proc. 13th ICRC (Denver) 5, 3202 and 3207.
——— 1974 talk, NATO Advanced Study Institute, Durham.
——— 1975, Proc. 14th ICRC (Munich) 2, 598.
——— 1977a, Research Proposal, unpublished.
——— 1977b, Proc. 15th ICRC (Plovdiv) 12, 56, 62, 89.
——— 1981 in Proc. IUPAP/IAU Symposium N° 94, Origin of Cosmic Rays, eds. G. Setti et al. (Reidel: Dordrecht) p. 53.
——— 1982 in Proc. Workshop on Very High Energy Cosmic Ray Interactions, eds. M.L. Cherry et al. (University of Pennsylvania: Philadelphia) p. 83.
——— 1983 in Proc. Cosmic Ray Workshop, University of Utah, ed. T.K. Gaisser (Bartol Research Foundation: Newark) p. 289.
——— 1983, Research Reports UNML-6/11/83, UNML-6/15/83 and UNML-6/20/83.
——— and Scarsi 1962, Phys. Rev. Lett. 9, 123.
——— and Watson 1977, Proc. 15th ICRC (Plovdiv) 12, 203.
—————— 1981, Phys. Rev. Lett. 46, 459 and Proc. 17th ICRC (Paris) 2, 137; 6, 238.
Lloyd-Evans, J. 1982 Thesis, University of Leeds.
Lloyd-Evans, J. and Watson, A.A. 1983, Invited Talks, 8th European Symposium, eds. N. Iucci et al. (Tecnoprint: Bologna) p. 81.
Lovelace, R.V.E. 1976, Nature 262, 649.
Markov, M. and Zheleznykh, I. 1979, Proc. DUMAND Workshop, ed. J. Learned (University of Hawaii: Honolulu) p. 177.
McIvor, J. 1977, M.N.R.A.S. 179, 13.
Michel, F.C. and Dessler, A.J. 1981, Proc. 17th ICRC (Paris) 2, 340.
Miura, I. and Hasegawa, H. 1962, J. Phys. Soc. Japan 17, Suppl. A-III, 84.
Müller, D. 1982 in Proc. Workshop on Very High Energy Cosmic Ray Interactions, eds. M.L. Cherry et al. (University of Pennsylvania, Philadelphia) p. 448.
Nikolskii, S.I. 1962, Proc. 5th Inter-American Seminar on Cosmic Rays, La Paz, eds. I. Escobar et al. (Lab. Fisica Cosmica: La Paz) 2, XLVIII.
——— 1975, Izv. AN SSRR, ser. fiz. 39, 1160.
Nikolskii, Kabanova, Stamenov & Janminchev 1979, Proc. 16th ICRC (Kyoto) 8, 335.
Ormes, J.F. 1982 in Proc. Workshop on Very High Energy Cosmic Ray Interactions, eds. M.L. Cherry et al. (University of Pennsylvania, Philadelphia) p. 466.
Orth, C.D., Buffington, A., Smoot, G.F. and Mast, T.S. 1978, Ap. J. 226, 1147.
Owens, A.J. and Jokipii, J.R. 1977, Ap. J. 215, 677.
Peters, B. 1960, Proc. 6th ICRC (Moscow) III, 157.
Peters, B. and Westergaard, N.J. 1977, Astrophys. Space Science 48, 21.
Puppi, G. 1956 in Progress in Cosmic Ray Physics, ed. J.G. Wilson (North-Holland: Amsterdam) Vol. 3, p. 338.

REFERENCES: PRE-CONFERENCE PAPERS - continued

Rasmussen, I.L. 1975 in Origin of Cosmic Rays, eds. J.L. Osborne and A.W. Wolfendale (Reidel: Dordrecht) p. 97.

Rossi, B. 1934, Supplemento a la Ricerca Scientifica 1, 579.

——— 1948, Rev. Mod. Phys. 20, 537.

Ryan, Ormes and Balasubrahmanyan 1972, Phys. Rev. Lett. 28, 985 & Erratum 1497.

Sakakibara, S. 1965, J. Geomag. Geoelectr. Japan 17, 99.

——— 1976, Proc. Intern. Cosmic Ray Symposium on High Energy Cosmic Ray Modulation, eds. K. Nagashima et al. (Tokyo) p. 316.

——— 1979, Proc. 16th ICRC (Kyoto) 4, 216.

Shapiro, M.M. and Silberberg, R. 1975, Phil. Trans. Roy. Soc. London A277, 319.

——— 1983, Ap. J. 265, 570.

Simon et al. (Goddard group) 1980, Ap. J. 239, 712.

Sokolsky, P. 1983, Proc. Cosmic Ray Workshop, University of Utah, ed. T.K. Gaisser (Bartol Research Foundation: Newark) p. 153/

Sood, R.K. 1983, Nature 301, 44.

Stamenov, J.N. and Ushev, S.Z. 1977, Proc. 15th ICRC 8, 133.

Stecker, F. 1979, Ap. J. 228, 919.

Strong, A.W., Wdowczyk, J. and Wolfendale, A.W. 1974, J. Phys. A 14, 1767.

Thornton, G. and Clay, R. 1979, Phys. Rev. Lett. 43, 1622 & Erratum, 45, 1463.

Vernov, S.N. & Khristiansen, G.B. 1968, Can. J. Phys. 46, S197.

Walker, R. and Watson A.A. 1982, J. Phys. G 8, 1131.

Wdowczyk, J. and Wolfendale, A.W. 1976, J. Phys. A 9, L197.

——— 1983 preprint.

Webber, W.R. 1958, Suppl. Nuovo Cimento 2, 532.

Williams, R.W. 1948, Phys. Rev. 74, 1689.

Wilson, J.G. 1956, Proc. Oxford Conference on Extensive Air Showers, ed. T.E. Cranshaw (Atomic Energy Research Establishment: Harwell) p. 1.

Wolfendale, A.W. 1977, Proc. 15th ICRC (Plovdiv) 10, 235.

Yodh, G.B. 1981 in Cosmology and Particles, eds. J.A. Adouze et al. (Editions Frontieres: Dreux)

Zatsepin, G.T., Nikolskii, S.I. and Khristiansen, G.B. 1963, Proc. 8th ICRC (Jaipur) 4, 100.